# Performance Characterization of Digital Optical Data Transfer Systems for Use in the Space Radiation Environment

Robert A. Reed, NASA-GSFC, Code 562, Greenbelt, MD and
Ray L. Ladbury, Orbital Sciences Corporation, McLean, VA

*To be presented at the*
*Nuclear and Space Radiation Effects Conference (NSREC) Short Course*
*Monday, July 24, 2000*

# Performance Characterization of Digital Optical Data Transfer Systems for Use in the Space Radiation Environment

Robert A. Reed, NASA-GSFC, Code 562, Greenbelt, MD and
Ray L. Ladbury, Orbital Sciences Corporation, McLean, VA

## 1.0 Introduction

Radiation effects in photonic and microelectronic components can impact the performance of high-speed digital optical data link in a variety of ways. This segment of the short course focuses on radiation effects in digital optical data links operating in the MHz to GHz regime. (Some of the information is applicable to frequencies above and below this regime) The three basic component level effects that should be considered are Total Ionizing Dose (TID), Displacement Damage Dose (DDD) and Single Event Effects (SEE). In some cases the system performance degradation can be quantified from component level tests, while in others a more holistic characterization approach must be taken.

In Section 2.0 of this segment of the Short Course we will give a brief overview of the space radiation environment follow by a summary of the basic space radiation effects important for microelectronics and photonics listed above. The last part of this section will give an example of a typical mission radiation environment requirements. Section 3.0 gives an overview of intra-satellite digital optical data link systems. It contains a discussion of the digital optical data link and it's components. Also, we discuss some of the important system performance metrics that are impacted by radiation effects degradation of optical and optoelectronic component performance. Section 4.0 discusses radiation effects in optical and optoelectronic components. While each component effect will be discussed, the focus of this section is on degradation of passive optical components and SEE in photodiodes (other mechanisms are covered in segment II of this short course entitled "Photonic Devices with Complex and Multiple Failure Modes"). Section 5.0 will focus on optical data link system response to the space radiation environment. System level SEE ground testing will be discussed. Then we give a discussion of system level assessment of data link performance when operating in the space radiation environment.

## 2.0. Brief Summary of the Space Radiation Environment and Basic Effects

Earth-orbiting and interplanetary spacecraft face a variety of radiation-related threats. Determining the survival probability of a spacecraft during its mission requires not just accurate ground-based test data for the device and a validated model for predicting the device performance in space from the ground-based data. It also requires accurate prediction of the space radiation environment. Although a complete description of the space-radiation environment is beyond the scope of this course, its importance demands that we give at least a cursory treatment here. An excellent description of the space radiation environment as well as the use, validity, and limitations of the relevant models thereof, can be found in [Bart-97].

The radiation environment encountered by a spacecraft depends on several factors. The path of the spacecraft relative to the planets, the level of solar activity and the mission duration determine the radiation levels incident on the spacecraft. The spacecraft's ability to shield sensitive components from radiation can be crucial in determining whether radiation effects will affect the functioning of those components. Finally, for military spacecraft, the threat of man-made radiation environments (not addressed in this course) can be an important consideration. Typically, these variables are used as inputs to computer codes that predict the space radiation environment encountered by a spacecraft and how this environment affects the spacecraft's mission.

There are two major components of the natural space radiation environment: the transient environment and that trapped by the magnetic fields of most planets. As might be expected, Earth's trapped radiation environment is better characterized than those of the planets. Our brief discussion of the radiation environment will focus on the naturally occurring radiation environment as it affects the performance of microelectronic and photonic devices in Earth-orbiting spacecraft. Deep-space missions passing near other planets, radiation dosimetry [Dyer-98] and man-made radiation environments are described elsewhere [Teag-72].

**Figure 2.1** is an artist's conception of Earth's radiation environment. The near-Earth trapped particle environment will be discussed first, followed by a discussion of the solar and galactic transient radiation environments. Next, we will give a brief discussion of the

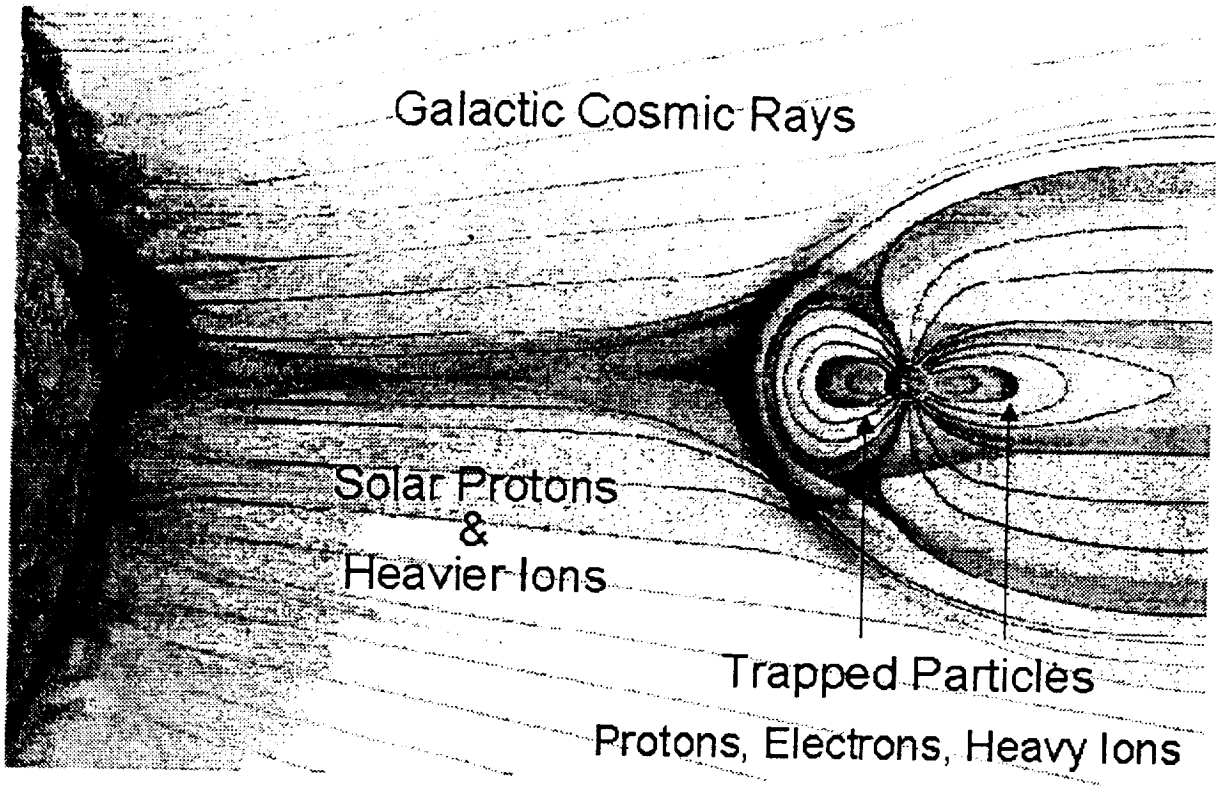


Figure 2.1. Cartoon showing the components of the space radiation environment that are important for microelectronic evaluation.

basic types of radiation effects in photonic and microelectronic devices. The last part of this section of the course will discuss the typical environmental data needed to evaluate and predict the performance of photonic and microelectronic devices exposed to the radiation environment.

## 2.1 Space Radiation Environment

The objective of this section is to give a brief summary of the radiation environment encountered by near-earth spacecraft. [Bart-97] gives a detailed description of the basic physics and theories that describe solar processes, Earth's magnetic field, charged particle interactions with the magnetic field and many of the other details not covered by this brief summary. The discussion is divided into two parts: trapped and transient radiation environments.

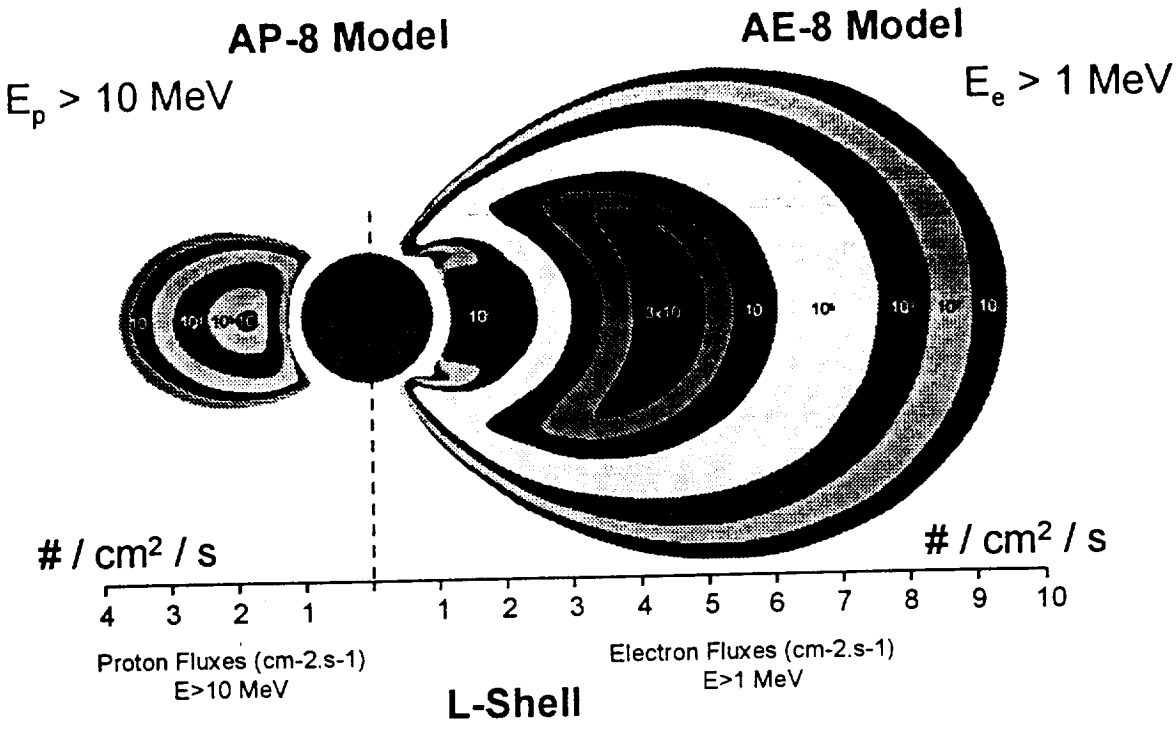


Figure 2.2. Artistic impression of the radiation belts surrounding the earth. The protons are depicted on the left and the electrons are depicted on the right.

### 2.1.1 Trapped Protons and Electrons

Particles with the proper charges, masses, energies and trajectories can be captured by the Earth's magnetic field. See [Barth97, Dyer98] for details of the species, origin, confinement processes, subsequent motion, and measurement of these particles. Of the particles confined by Earth's magnetic field, electrons and protons have the greatest effect on spaceflight hardware. **Figure 2.2** is an artist's impression of these two environments. The proton environment is given on the right side of the cartoon, and the electron environment is shown on the left. In simplified approximations of these environments, they form a toroid with Earth at the center and Earth's magnetic pole defining the toroid's central axis. (The geographic pole is roughly 11 degrees off center from the magnetic pole.)

As shown in the figure, the proton flux is confined to a single toriod, and electrons form two high intensity toriods. The region between the two electron zones is known as the slot region. Earth's atmosphere and magnetic field and their interaction with the solar

wind and the solar magnetic field define the details of the flux of each particle toriod. The particles roughly follow Earth's magnetic field lines.

In the inner region, L < 3.5, electron and proton toriods overlap, while for 3.5>L>8.5, the trapped particles are mostly electrons. No significant particle trapping occurs for values of L>8.5. In the trapped regions the flux is considered to be omnidirectional.

Although **Figure 2.2** presents a static view of the shape, regional flux, and orientation of the toriods, in reality, these belts are very dynamic, growing and shrinking over time. Occasionally, new torroidal regions form and disappear. The dynamic nature of the trapped radiation belts is not very well understood. Research has shown that fluxes can change dramatically with solar activity, but quantitative measurements of this variability still need to be refined.

One temporal variation that has been quantified is the variation of the flux levels in the toriods with the 11 year solar cycle. (During solar maximum the integral fluences for protons are lower than during solar minimum, while for electrons the reverse is true) It is the short duration temporal variation that are the most difficult to quantify.

Another modification to the simple toriodal model results from the fact that Earth's magnetic field is multipolar in nature, causing the magnetic field strength contours to sink towards the earth. This results in the South Atlantic Anomaly (SAA)—a dip towards the earth in proton and inner electron flux contours over the South Atlantic. For equal altitudes, the particle flux will be higher for locations in the SAA than for those outside of it.

The current approaches to modeling the trapped environment are given in [Bart-97, Hous-98, Xaps-98]. For example, the NASA AP8 and AE8, Huston-Pfitzer, CRRESPRO and CRRESELE models are used to model the trapped proton and electron environments.

### SRE.1.1 Trapped Heavier Ions

Ions with Z > 1 can also be trapped by Earth's magnetic field, although the intensities for these ions are lower than those for protons and electrons. The trapped heavy ions have energies on the order of 10s of MeV/amu, so most of them will not penetrate even the thinnest spacecraft shielding [Bart-97]. Effects of these particles on microelectronic and photonic systems are second order in most cases.

### SRE.1.2 Transient Environment

Although many types of radiation make up the transient environment, the two most important components for spacecraft electronic systems are the Galactic Cosmic Rays (GCRs) and particles emitted during solar particle events.

The sources of GCRs are sufficiently far from our solar system that the fluxes of these particles are essentially isotropic in free space regions. Interactions in the vicinity of Earth between the solar wind and our planet's magnetic field change individual particle trajectories and energies. However, the net GCR flux can is still essentially omnidirectional.

The GCR particle composition is roughly 83% protons, 13% alpha particles, 3% electrons, and 1% heavier ions ($Z > 2$). The ion energies range from 10s of MeV/amu to 100s of GeV/amu and beyond, and most ions are fully ionized. Some of these ions have sufficient energy to penetrate most shielding provided by a spacecraft structure. In [Bart-97], there is a complete description of the GCR environment, including relative abundances and energy spectra.

Not all of radiation impinging on Earth originates from such distant sources. The Sun can be thought of as a boiling pot of plasma that emits or accelerates charged particles most of the time. When the Sun is "quiescent", most of the particles it emits do not have sufficient energy to penetrate through even a small amount of spacecraft shielding. However, during times of high activity, the Sun emits and/or accelerates a spectrum of charged particles with a large range of energies for varying amounts of time. The duration of each event is usually between a few days and a week. The average frequency of these solar events varies roughly sinusoidally with the eleven-year sunspot cycle. **Figure 2.3** illustrates this variation over the last three solar cycles—showing the solar proton integral fluences (the spikes) over a thirty-year period superimposed over the sunspot numbers (smooth curve).

Two important classes of events that occur during this high activity period are Coronal Mass Ejection (CME) and solar flare. CMEs have been correlated with events that have a high probability of producing particles that reach the Earth. No such correlation has been observed for solar flares. Protons tend to be the dominant charged

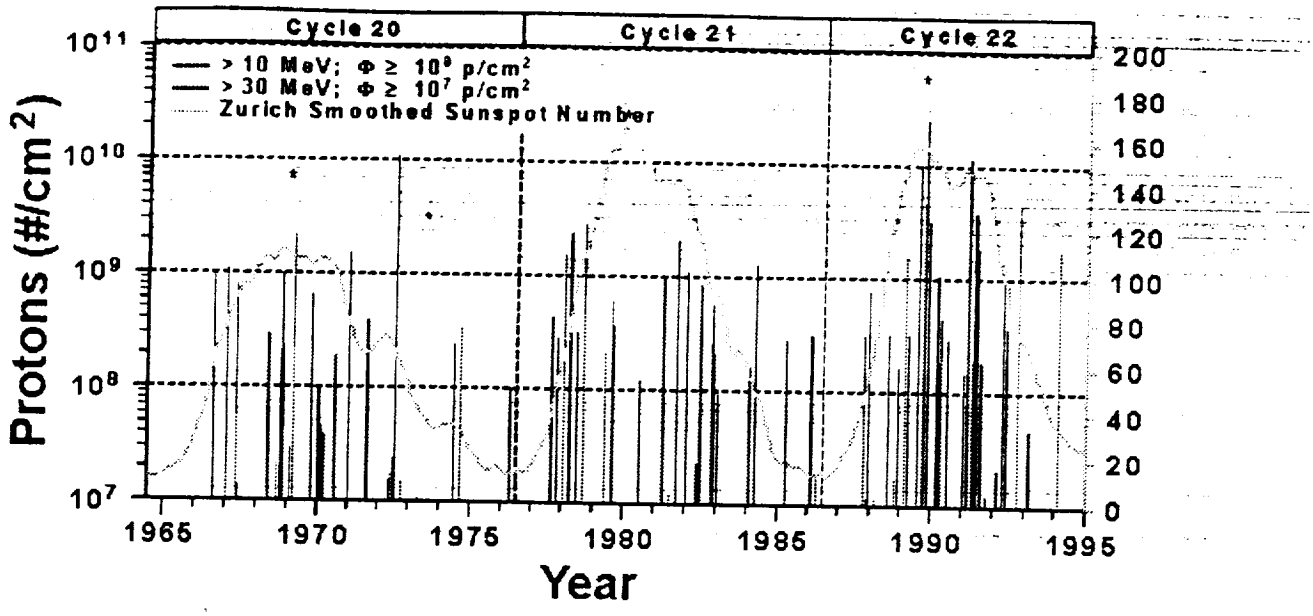


Figure 2.3. Solar particle events over a thirty year period (vertical light lines) compared to the sun spot number over time (single solid dark line).

particle for most of the solar events, but for some rare events with very high intensity, the particle spectra contain all naturally occurring elements (Z=1-92). The total integral fluences during these rare events can exceed average GCR fluxes by three orders of magnitude and more. Again, the reference of choice that describes the solar event environment in detail is [Bart-97].

## 2.2 Basic Radiation Effects

Microelectronic and photonic components are manufactured in very controlled environments. During certain phases of the manufacturing process, even the slightest change in conditions like temperature or impurity concentration can induce changes on the molecular level that cause the component to fail functional or parametric performance metrics. The point here is that devices that rely on such carefully grown, well-defined microscopic structures can have very low tolerance for slight changes in their characteristics. When a component is exposed to radiation, the radiation transfers some of its energy to the molecules of the component, changing the localized material properties. This can have significant effects on component functionality and/or parametrics

depending on the type of radiation, where the energy deposition occurs, and the type of component.

Three important effects that occur when a component is exposed to radiation are: Single Event Effects (SEEs), Total Ionizing Dose (TID), and Displacement Damage Dose (DDD). This section of will briefly define these effects and describe the basic interactions that cause the effect. It does not attempt to completely describe the impact that these basic interactions have on the performance of the transistor, microcircuit, or component. The reader will find detailed descriptions and discussions of the effects in other portions of this short course, past short courses, and in the many years of work published in the IEEE Transactions on Nuclear Science. Because a majority of this segment of the short course is dedicated to single event transient effects, these will be treated and described in more detail.

### 2.2.1 Single Event Effects

Ionizing radiation generates electron-hole pairs as it passes through a material. In an active device, these charges are swept up by the intrinsic and applied fields. If sufficient charge is collected at a sensitive junction, a variety of single-event effects can occur, with consequences ranging from trivial to catastrophic [for example see Dodd-99]. Single-event effects that can result in potentially catastrophic failures include single-event latchup (SEL) in CMOS, single-event gate rupture (SEGR) in power MOSFETs, single-event burnout (SEB) in FETs and bipolar transistors, single particle-induced failures of linear bipolar devices, and so on. If the collected charge results in a permanent logic change in the device (that is, a bit flip), the event is called a single-event upset (SEU). Alternatively, if the device merely changes its output state temporarily, the event is called a single-event transient.

Generally, the variable of choice used to characterize SEE is linear energy transfer (LET), which can be looked upon as the energy a particle loses as it passes through a medium normalized to the medium's density—$1/\rho * dE/dx$ (expressed, for example, in MeV*cm2/mg). Equivalently, for a given medium, LET can also be expressed as the charge generated per unit length of track (for example, pC/μm). In general, the higher LET a particle has—or, equivalently, the denser its charge track—the higher the

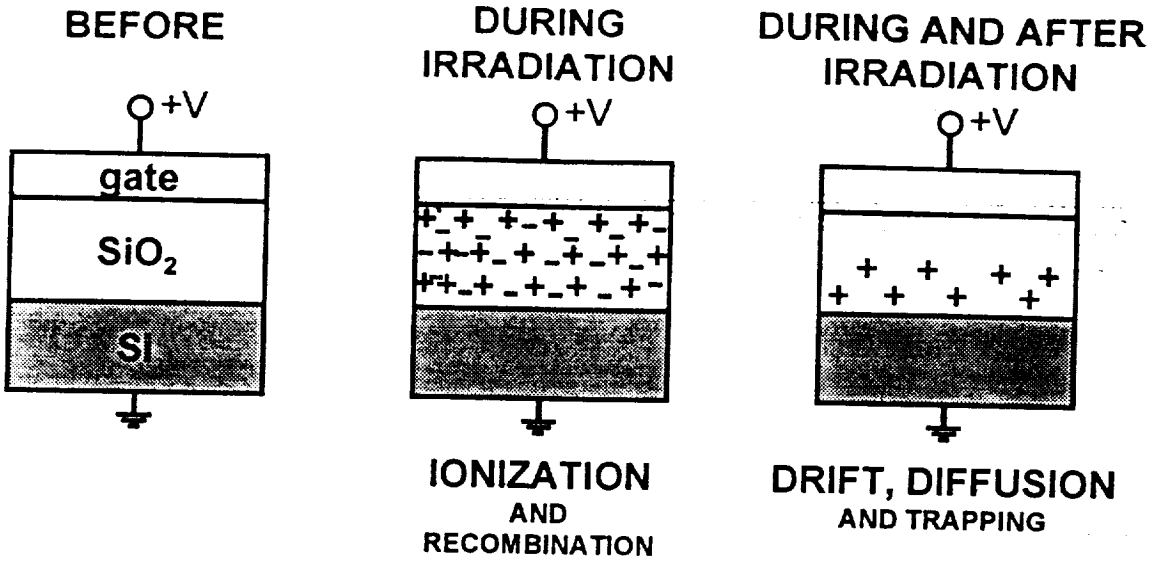


Figure 2.4. Simple model of generation and trapping of charge in an MOS device oxide. [Leray99].

probability that it may bring about a given SEE in a susceptible device. As in nuclear physics, the probability of a given effect is expressed as a cross section, with dimensions appropriate to the device ($\mu m^2$ or $cm^2$). In general, a device's cross section for a particular effect is related to the physical area on the device that is susceptible to the effect. However, the relationship is usually not a simple one.

Because optoelectronic devices may contain any traditional electronics technology, it should be remembered that they could be susceptible to any of these single-event effects. In addition, the optical components in these devices—particularly the detectors—may be susceptible to their own effects, especially SETs, which we will consider later.

### 2.2.2 Total Ionizing Dose

As with single-event effects, damage from TID is caused by the electron-hole pairs generated by ionizing radiation passing through a material. These charges can gradually change the performance of an electronic component, with the level of change depending on the total ionizing energy absorbed—that is, on the TID [Dres-98]. Generally, TID changes the characteristics of the materials that make up a component, resulting in gradual parametric degradation and changes in functionality. In most cases, the basic cause of TID degradation is the trapping of charge in the medium. **Figure 2.4** illustrates

a simple model of generation and trapping of charge in the dielectric of a MOS device with a positive bias applied to the gate. If enough charge is trapped in the oxide, the device's performance will change [Dres-98]. Charge may also be trapped in the field oxide of a linear bipolar device [Peas-96]. A third example would be the charge trapped in an optical fiber, a topic that we will discuss later.

### 2.2.3 Displacement Damage Dose

The proper functioning of many devices depends critically on the semiconductor having a pristine crystalline lattice. However, this lattice can be damaged when an energetic particle, such as a neutron, electron, proton or heavy ion displaces one or more nuclei within the crystalline lattice, creating electrically active defects. As this damage to the crystalline lattice—called the displacement damage dose (DDD)—increases, the device can degrade parametrically, and eventually stop functioning all together.

For the most part, because protons are penetrating, strongly interacting and abundant, the proton environment is predominant in considerations of DDD effects in shielded applications. However, for lightly shielded applications, low-energy electrons may also need to be considered. Moreover, for heavily shielded applications, secondary products can also be an important component of the environment. [Mars-99] and segment II of this short course explores DDD effects.

## 2.3 Case Study: Environment Predictions for a Near-Earth Spacecraft

The primary science objective of the Guided Laser Altimeter System (GLAS) instrument is to obtain day & night, long-term ice-sheet topography measurements with sufficient spatial and temporal resolution to detect regional elevation changes. The GLAS instrument will be placed in a polar orbit over the Earth at an altitude of 600 kilometers. The altimetry subsystem of the instrument uses a high-powered laser and sophisticated optical receiver to detect the outgoing laser pulse and the return signal reflected from the Earth.

The radiation environment encountered by the microelectronics and photonics on GLAS is a combination of the primary space environment and a secondary environment. The secondary environment is produced when the primary environment interacts with

spacecraft materials. For the most part, the primary environment dominates. Although this is true for most spaceflight missions, when heavy or composite shielding is used, one must carefully consider the secondary component of environment inside a spacecraft. An accurate description of the space environment for a specific mission can be crucial when developing an appropriate survivability test plan for microelectronic and photonic components.

This section of the Short Course describes the radiation environment for a spacecraft in a polar orbit at 600 km above Earth's surface. The description focuses on the environments that are important for most microelectronic and photonic devices. The minimum shielding considered is 50 mils of aluminum. Combining these environment predictions with accurate ground testing results, one can estimate the effects of space radiation on microelectronic and photonic components.

### 2.3.1 SEE Environment

Single-event effects can occur via either direct or indirect ionization. Direct ionization is produced by a primary ionizing particle interacting directly with charges (mainly electrons and holes) in the semiconductor. The direct-ionization environment is characterized by the integral LET flux distributions. Indirect ionization is a two step process. First, a primary particle interacts with a nucleus in the semiconductor lattice, producing one or more recoiling ions. These recoiling ions then produce ionization in the medium. Because protons are by far the most numerous particles capable of producing nuclear interactions, the indirect ionization is described by the integral flux curves for protons.

The integral LET flux curves reflect the combined direct ionization effects for all particles (Z = 1 to 92) from all sources. The major sources are the GCR background environment and the environment resulting from solar particle events. **Figure 2.5** depicts eight curves showing the heavy ion (Z=1-92) LET spectra for these two sources (as computed by CREME96), assuming different aluminum-shielding thicknesses. The bottom four curves are the GCR background environment. Notice that shielding has little effect after the first few mils of equivalent aluminum.

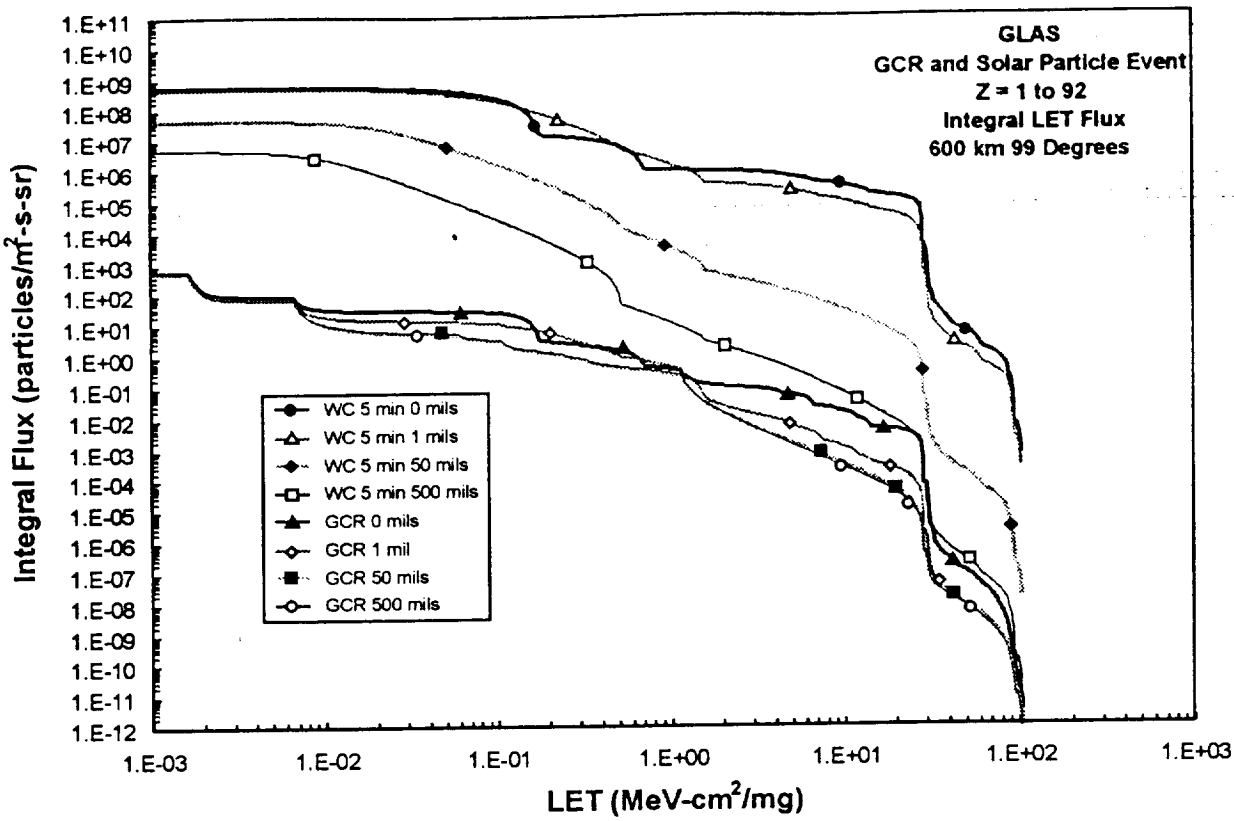


Figure 2.5. Integral LET heavy ion and solar proton flux spectra.

The four top curves are for the worst case 5 minutes during an anonymously large solar particle event. Notice that these particle fluxes are strongly dependent on shielding thickness. Because such large solar events are quite rare, these curves should only be used to determine the peak SEE rates.

**Figure 2.6** shows the LET spectra for the trapped proton environment for four shielding thicknesses. Direct ionization effects from protons are rarely of concern for SEEs. However, as we will discuss later, for certain devices, direct ionization from protons can contribute significantly to probability of SETs.

**Figures 2.7** and **2.8** give the integral flux over all energies for the trapped protons and protons from solar particle events for four shielding thicknesses.

### 2.3.2 TID Environment

The total ionizing dose environment is a combination of several components of the natural occurring space environment. **Figure 2.9** shows each component and the total for

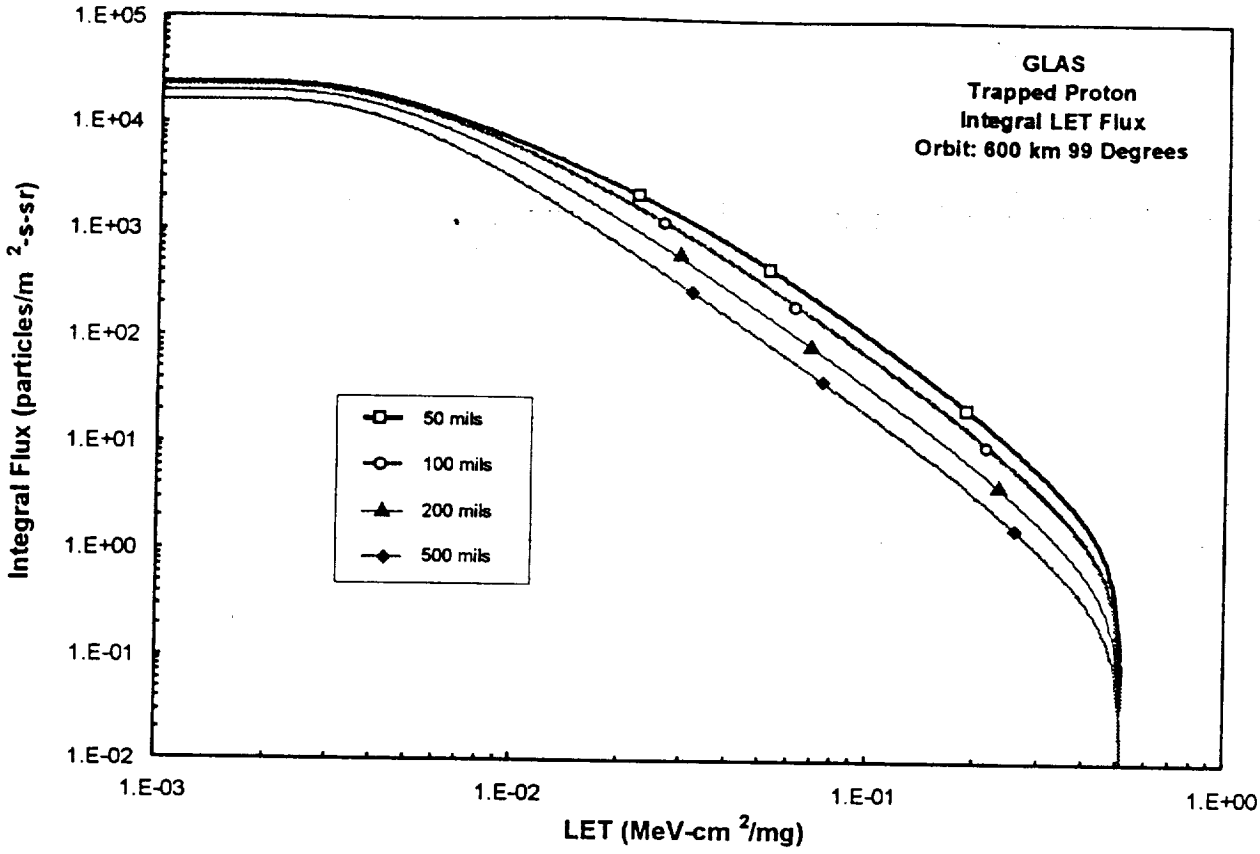


Figure 2.6. Integral LET Trapped proton flux spectra.

silicon. The total ionizing dose is simple a summation of all the components, with trapped electrons, bremstrahlung, trapped protons, and solar particle event protons being the main contributors.

### 2.3.3 DDD Environment

Section II of this Short Course gives a complete description of the important issues to be considered when determining the DDD environment. We mention this effect here only for completeness. The major contributors to DDD when considering most applications of microelectronic and photonic components are the trapped and solar protons. **Figures 2.10** and **2.11** give the differential flux over all energies for the trapped protons and protons from solar events for four shielding thicknesses. The details of how to compute the DDD from these data are given in Section II of this Short Course.

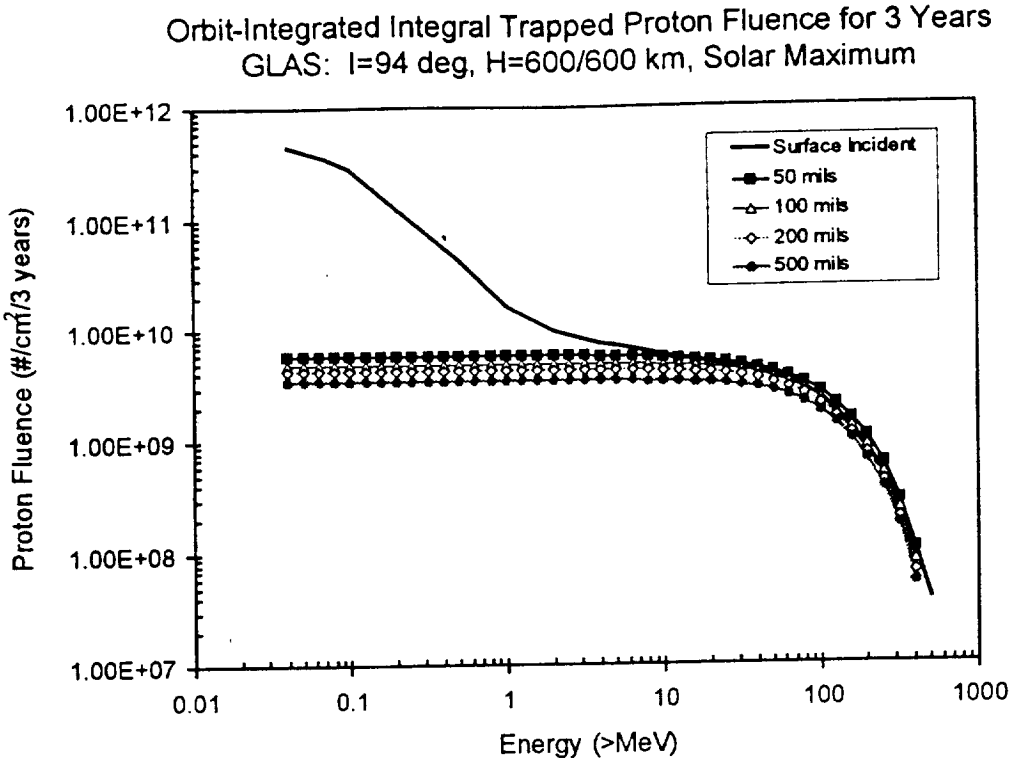


Figure 2.7. Orbit integrated trapped protons fluence.

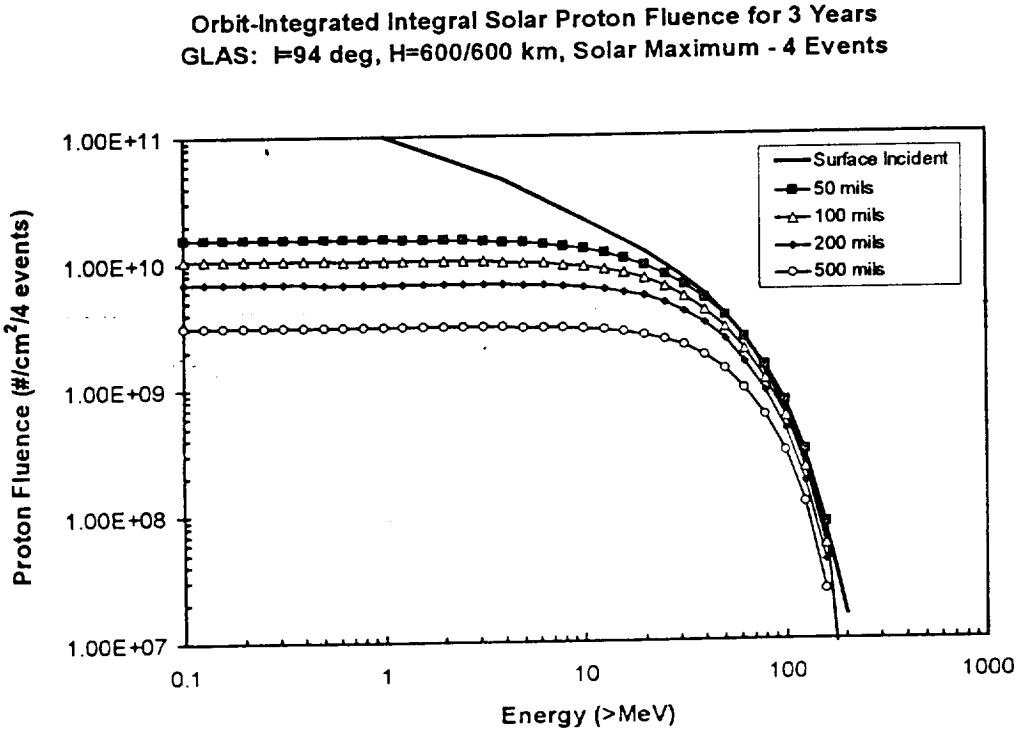


Figure 2.8. Orbit integrated solar proton fluence.

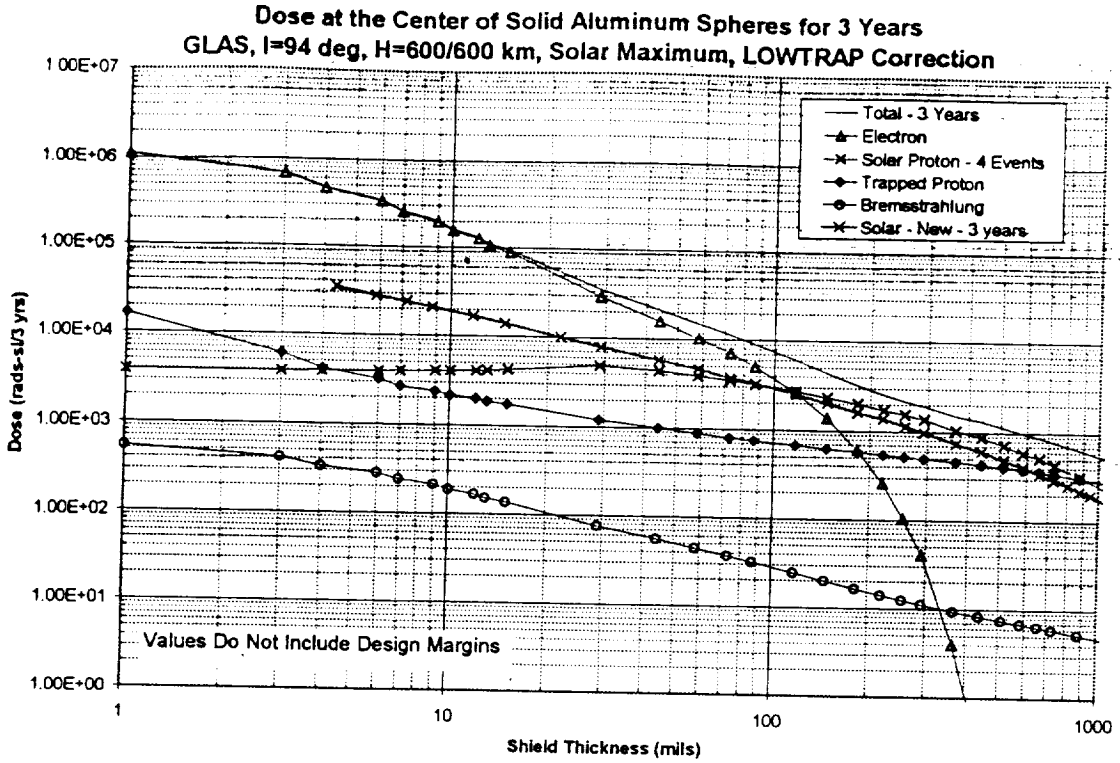


Figure 2.9 Dose curves for various components of the spectra for various shielding thickness.

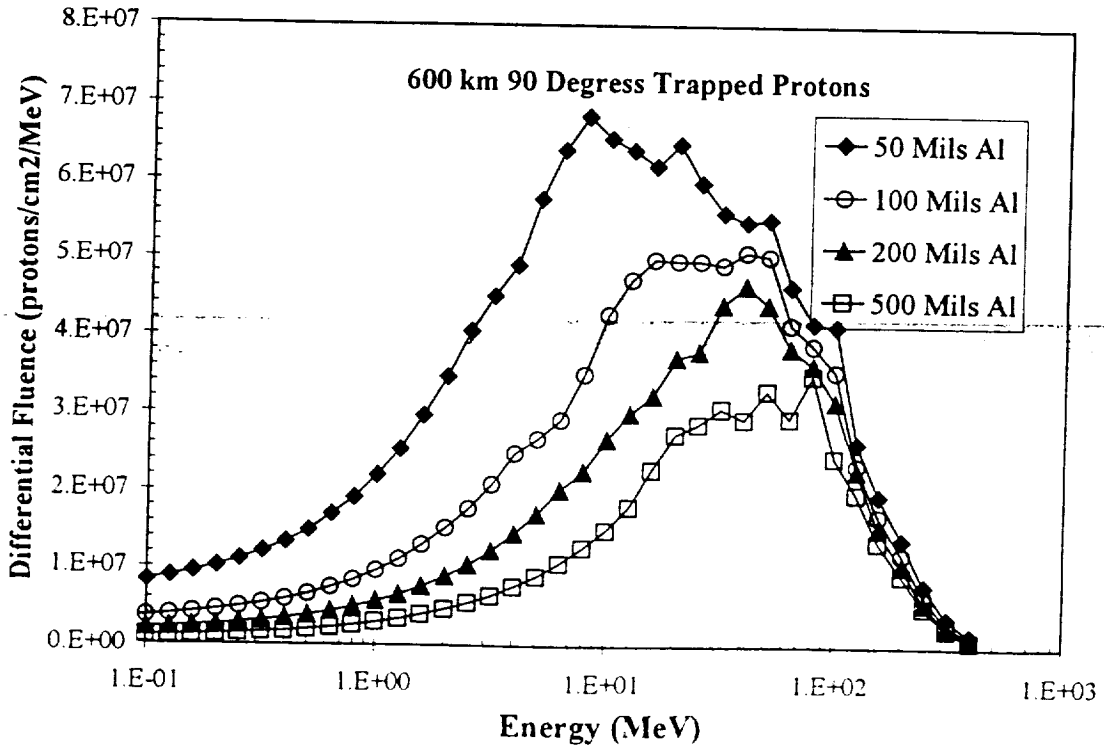


Figure 2.10 – Trapped proton differential spectra.

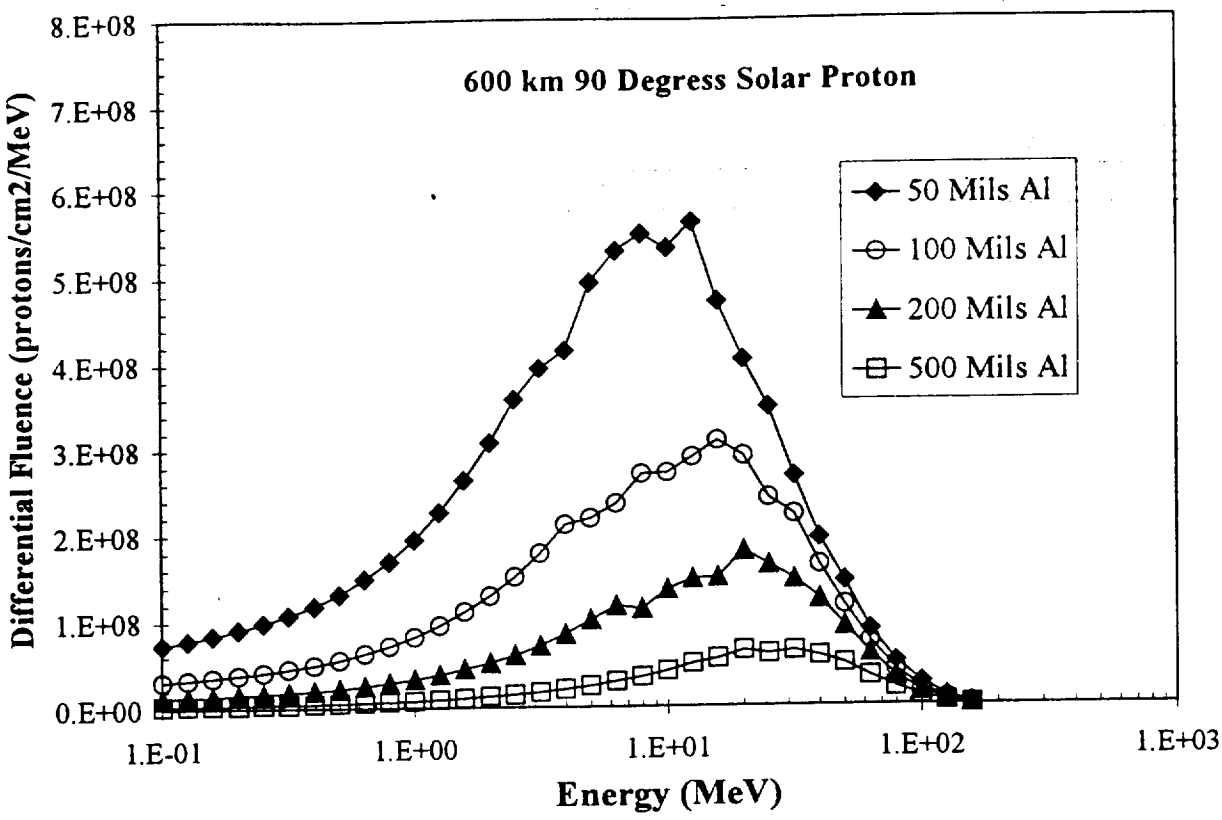


Figure 2.11 – Solar proton differential spectra.

## 3.0 Intra-Satellite Digital Optical Data Link

In the search of high-bandwidth digital data transfer systems, spacecraft designers are considering high-speed digital optical links as an alternative to the conventional systems. Designers must determine the best link for the mission based on performance metrics of each data link. The focus of this Short Course is to give the designer a clearer understanding of the radiation effects in optical data links and how those effects affect link performance.

This section introduces digital optical links by giving a general description of optical data transfer systems with a brief overview of each component of the optical portion of a fiber-optic data link. The optical system performance metrics important when characterizing performance degradation due to radiation exposure are also discussed. Several excellent books on fiber-optic data links are listed at the end of the chapter, most of the material present in this section is a summary of taken from these books [Agra-97, Pala-98, DeCu-98, and Lach-98].

### 3.1 Overview of the Digital Optical Data Link

Data links transmit large amounts of information at high data rates between spacecraft subsystems. Classically this is done via an electrical connection using standardized data link hardware, **i.e., RS232 and MIL-STD 1553.** Data transfer at rates in the MHz to GHz range can also be achieved using optical data links, where optical fiber and its associated components are used in place of wire and its components. Some of the advantages and disadvantages of optical systems are listed **Table 3.1**. A detail comparison of optical versus electrical data links is beyond the scope of this Short Course. However, it is obvious from the list of advantages that, for many applications, optical links should be considered as a serious option.

Table 3.1 List of some of the advantages and disadvantages of fiber link systems.

| Advantages | Disadvantages |
|---|---|
| Wide bandwidth | Potential cracking of fiber |
| Light weight | Limited fiber bending radius |
| Reduced complexity during spacecraft integration | |
| Immunity to electromagnetic interference | |
| Elimination of cross talk | |

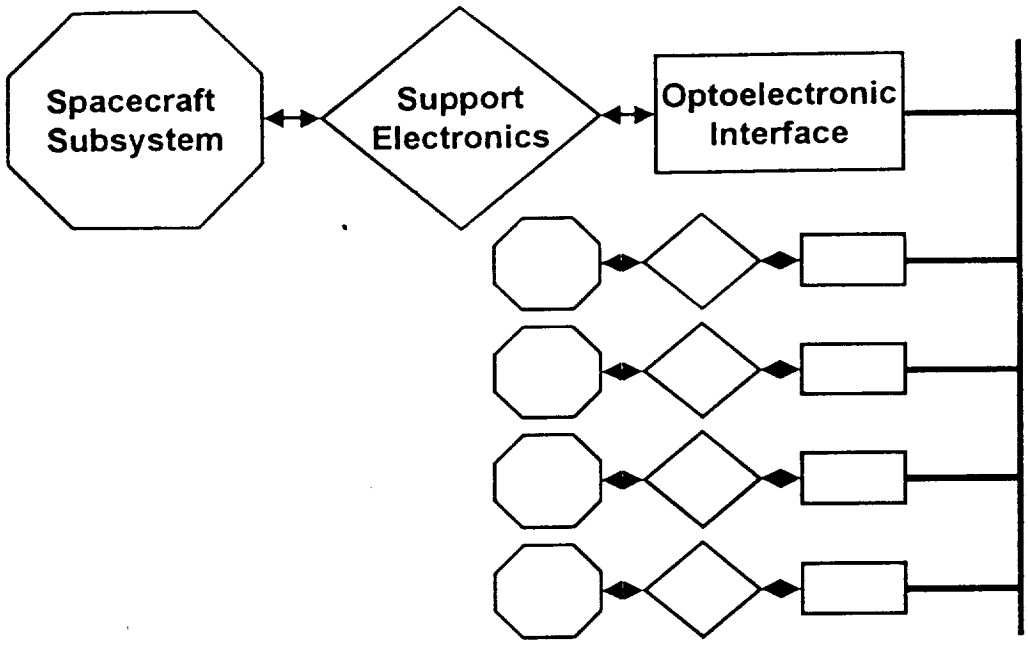


Figure 3.1 Block diagram of fiber-optic data transfer interface between spacecraft subsystems.

**Figure 3.1** shows a typical optical data link system. Digital data flows from subsystem to subsystem via optical fiber. The support electronics condition the signal, optoelectronics convert the signal between optical and electrical formats. In the next few sections different network architectures will be discussed followed by a discussion of the optoelectronics portion of the network (a detailed discussion of each component will be given in section 3.2)

### 3.1.1 Network Architectures

The network architecture is the baseline for how each subsystem is connected to all the other subsystems on the network. Four popular topologies are given in **Figure 3.2** 1) point to point, 2) linear bus 3) star hub and 4) ring.

The point to point network (**Figure 3.2.A**) is two subsystems are link via a single optical fiber. Each subsystem can communicate only to its partner through a single optical fiber. The fiber is a single point failure, this is avoided by using redundant data paths.

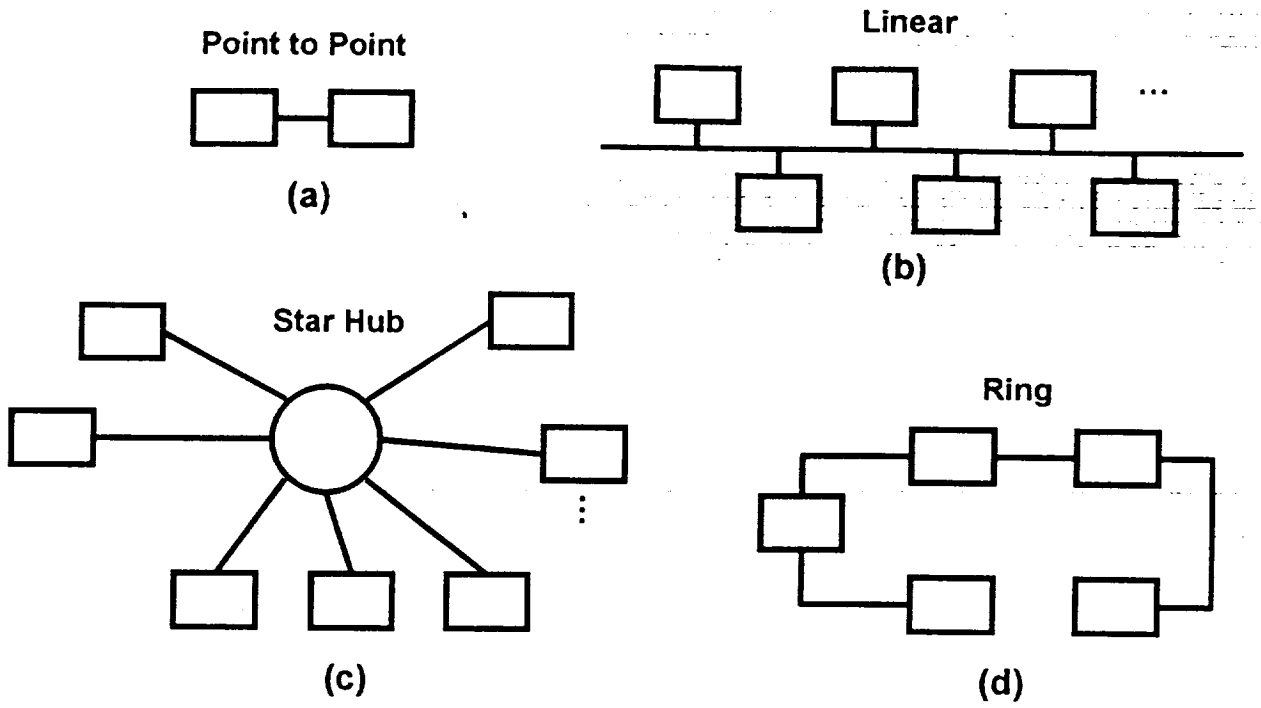


Figure 3.2. Four common network topologies.

The optical power that is required to support the data link is one of the major factors in determining which network topology to use in a spacecraft design. For example comparing the last three networks in **Figure 3.2**, the ring and the star hub has an inherent lower optical power loss as the signal passes from subsystem to subsystem [Agrawal97]. First consider the linear bus configuration. The power reaching a specific subsystem is used increases exponentially with the number of subsystem between the transmitting subsystem and the receiving subsystem. While in the star hub the power at the receiver decreases linearly with the number of subsystems on the hub. As we will see later, there is a relationship between radiation exposure degradation of network optical power and data link performance.

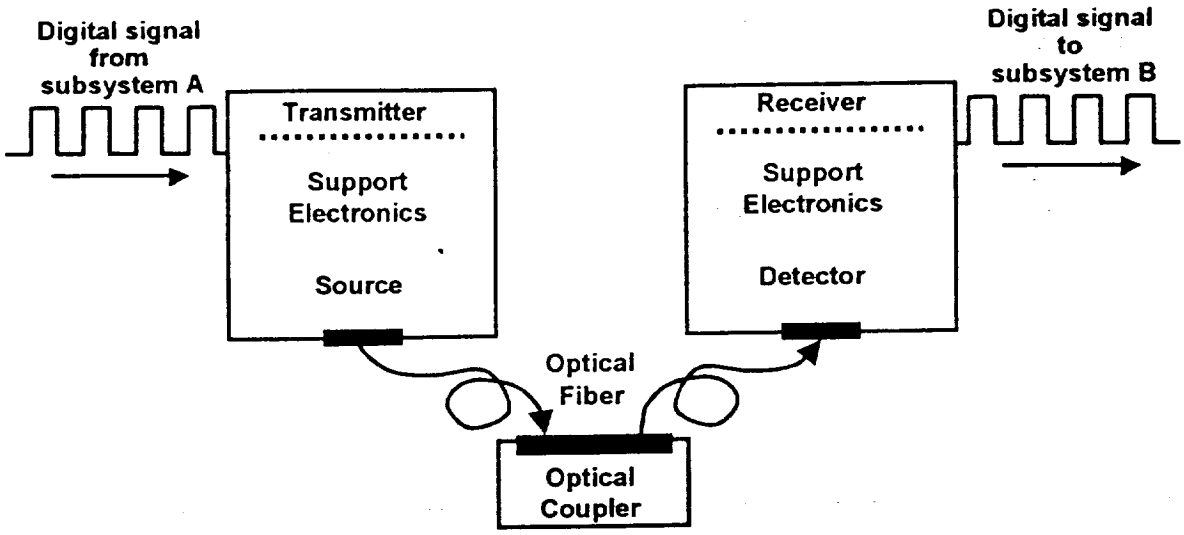


Figure 3.3. Block diagram of simple point to point architecture.

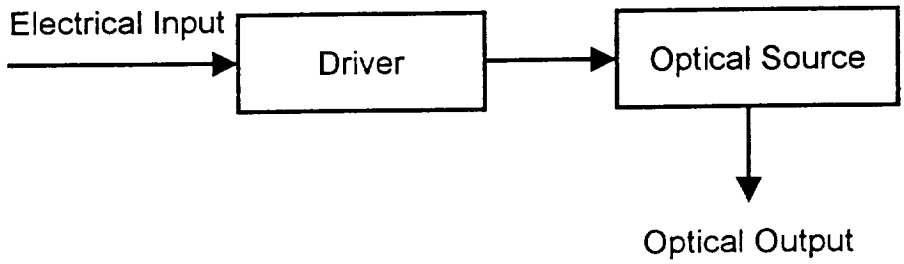


Figure 3.4. Block diagram of an optical transmitter

### 3.1.2 The Optical Data Link

**Figure 3.3** is a cartoon of two subsystems connected via an optical data link. The digital data is passed from the subsystem A to the transmitter, through an optical medium, then to the receiver, and finally to subsystem B electronics.

The transmitter's function is to convert the electrical signal into an optical format and launch the optical signal onto the fiber. **Figure 3.4** gives a block diagram of an optical transmitter.

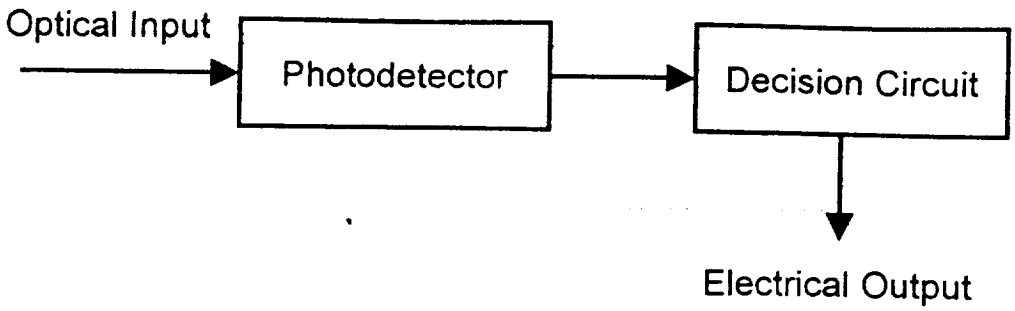


Figure 3.5. Block diagram of an optical receiver

The optical light source output power is an important parameter that is expressed in units of dBm where to optical output power is referenced to 1 mW. In general, to convert from power in Watts to power in dBm use:

$$\text{Power (dBm)} = 10 \log_{10} \left( \frac{\text{Power}}{1 \text{ mW}} \right) \qquad \text{(Eq 3.1)}$$

So a source that launches 0 dBm is a 1 mW source. Power loss is defined as the difference between the launched and received power in dBm. The units for power loss are dB.

Optical fiber transfers the optical signal from the transmitter to the receiver. The goal is to select fiber that minimizes signal distortion. Loss and dispersion of the optical signal due to optical fiber are important considerations when selecting the optical fiber.

The optical receiver converts the optical signal launched by the output end of the optical fiber back into the electrical signal. **Figure 3.5** is a block diagram of an optical receiver. The optical signal is detected by the photodetector, its output current is related to the intensity of the optical signal. The decision circuitry identifies the value of the data bit by comparing the resulting output voltage level induced by the current flow in the photodetector to a reference voltage.

In some data link designs there are a large number of microelectronic devices that support the transmitter and receiver sides of the data link. These support electronics may include voltage level shifters, MUX, DeMUX, encoders, decoders, shift registers, phase lock loops, and a host of others.

Section 3.2 describes in more detail some of the components that form the optical link. We will focus on the key components that are specific to optical data links. (Section 4.0 we will discuss the radiation effects concerns for these components.)

### 3.2 Brief Description of Optical Link Components

The last section gave an overview of the optical data link, in this section we will focus on the components that make up such a link. The discussion is confined to components that are unique to optical data links. Namely light sources, optical fiber, and receivers (emphasis on photodetector portion). Support electronics will not be discussed in detail.

#### 3.2.1 Optical Transmitter

In this section we review transmitters used in fiber-optic data links. Transmitters contain a drive circuit and a source, see **Figure 3.4**. Typically, LEDs and laser diodes are used as light sources. The driver converts the input electrical signal to a current. Source modulation is achieved by varying the injection current (It is also possible to modulate the light output directly, however this is not as common as injection current modulation). Sometimes, a lens (not shown) is used to couple the output light to the optical fiber. Optical sources will be described in below. Segment II of the short course will give details of source operation along with the detail discussion of the radiation effects mechanisms. Also, most any text on fiber-optic communications, for example Agrawal97, will give a detail discussion of optical sources.

Semiconductor light sources, either Light-Emitting Diodes (LEDs) or laser diodes, are used as sources for fiber-optic data links. These devices have very suitable characteristics for use in fiber-based links, e.g. size, range of wavelengths, and power consumption. Sources are classified as long-wavelength or short-wavelength sources. Short-wavelength sources operate in the 500-1000 nm and are typically a ternary blend of semiconductors, e.g. GaAlAs. Long-Wavelength sources produce light from 1200-1600 nm and are typically quaternary semiconductors like InGaAsP. A well confined forward-biased pn junction forms the region in the semiconductor where light is emitted.

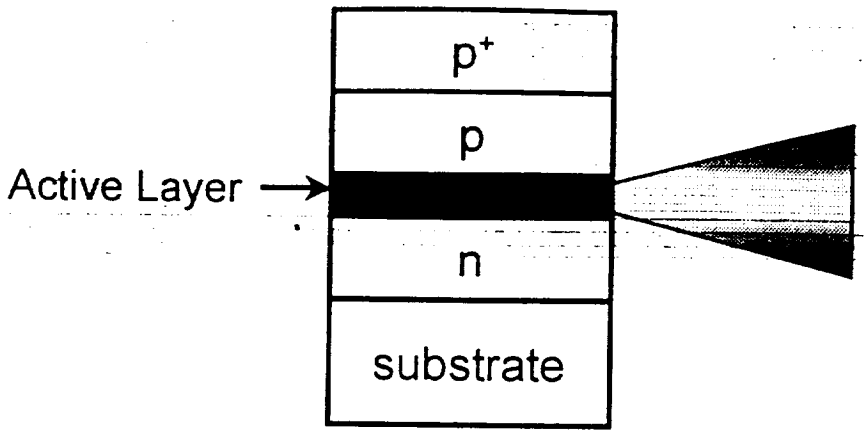


Figure 3.6. Light emitting device showing active layer where current and light confinement occurs.

### 3.2.1.1 Semiconductor Light Emission and the Resulting Wavelength

Forward biasing a pn junction causes holes to be injected into the n-doped region and electrons to be injected into the p-doped region. These injected minority carriers are free to recombine with the majority carriers. Energy of the charge-carrier pair is given off during the recombination process as electromagnetic radiation (photons) or heat. When light is generated this is called radiative recombination. Internal quantum efficiency, $\eta_{int}$, is defined as the fraction of recombinations that are radiative. Not all recombinations are associated with emission of light, some recombination are nonradiative.

Light emitted from LEDs is known as spontaneous emission, it is randomly directed, incoherent, and randomly polarized. Laser diodes use a stimulating light wave to initiate light emission. The light is polarized, coherent and in the same direction.

As current carrier concentration increase the radiative recombination efficiency goes up [Cheo-90]. Therefore it is desirable to confine current flow to the active region in a light emitting device, **Figure 3.6.** Some devices are fabricated such that electrons injected into the active region from the n-type region will see the p-type region as an energy barrier, likewise holes injected into the active region face an energy barrier from the n-type region. This type of boundary is known as a double heterojunction structure. Another feature of the heterojunction diode is that the different index of refraction serves to confine the light to the active region which reduces absorption of light in the semiconductor and increases the output power of the diode.

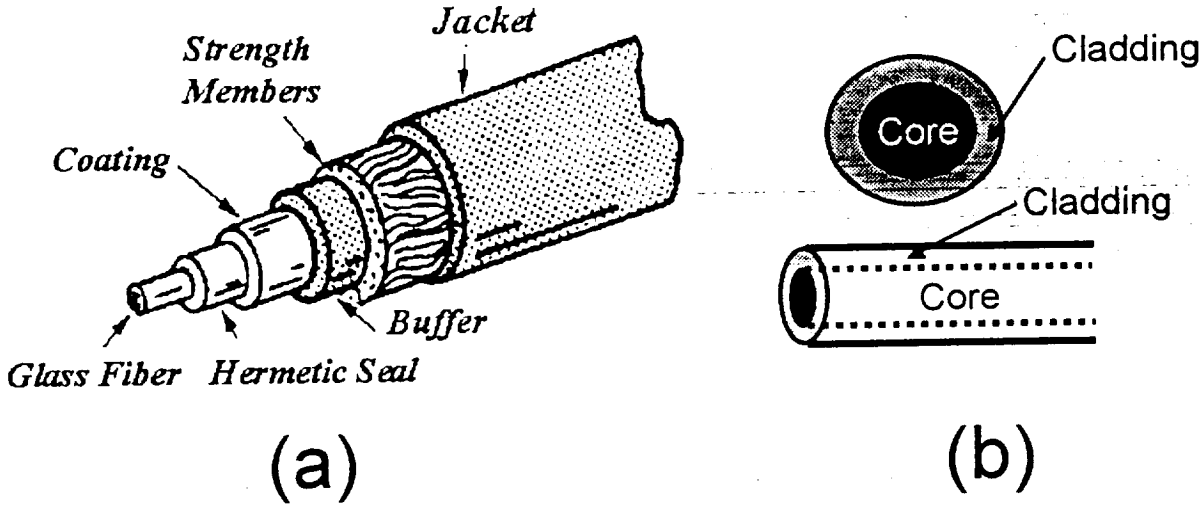


Figure 3.7. (a) Typical optical fiber housing. (b) Shows core and cladding.

During radiative recombination the photon energy is equal to the band-gap energy ($E_g$) of the semiconductor. It will have a wavelength ($\lambda$) defined by :

$$\lambda = \frac{hc}{E_g} \qquad \text{(Eq 3.2)}$$

h is Planck's constant ($6.63 \times 10^{-34}$ joules sec) and c is the speed of light.

### 3.2.2 Optical Fiber and Other Passive Components

Fiber optic waveguides confine light within a long strand of glass. **Figure 3.7.A** shows a typical optical fiber housed within several protective layers. The optical fiber itself consists of a core and a cladding, **Figure 3.7.B.**

The fiber core and cladding act to confine the light by internal reflection at the core-cladding interface. Optical fibers are manufacture so that the core has a higher index of refraction than the cladding. The index of refraction (n) is defined as:

$$n = \frac{c}{v} \qquad \text{(Eq. 3.3)}$$

where c is the velocity of light in a vacuum and v is the velocity of light in the medium. Using Snell's law (see segment II of this Short Course) shows that for a certain combinations of core ($n_1$) and cladding ($n_2$) there is a specific critical angle (measured

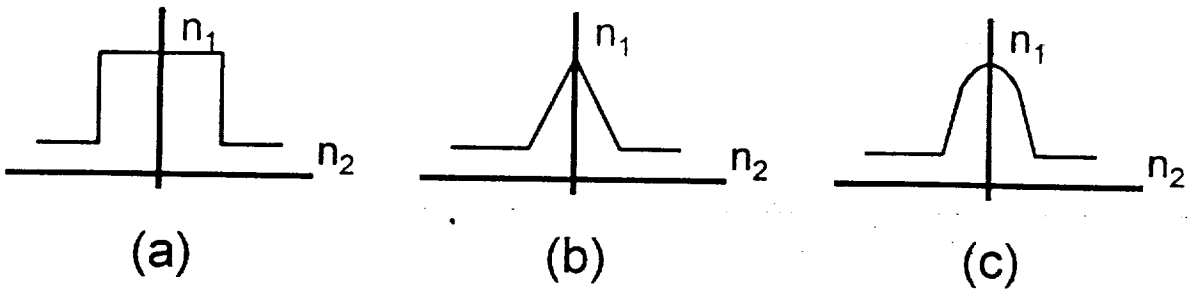


Figure 3.8. Variation in the index of refraction profile moving from the center the core to the cladding. (After Agrawal92)

from a line perpendicular to the core-cladding interface). If the angle of incidence of the light traveling in the core is less than the critical angle then some of the light will be transmitted into the cladding. The critical angle is found from:

$$\mathrm{Sin}(\theta_c) = \frac{n_2}{n_1} \qquad \text{(Eq. 3.4)}$$

Optical fiber can be fabricated to have an index of refraction that changes abruptly at the core-cladding interface, these are known as step-index fibers (**Figure 3.8.A**). Other fibers have a triangular profile (**Figure 3.8.B**) or a graded-index profile shown in **Figure 3.8.C**. While yet other fibers may have various discreet steps in index of refraction. Each profile gives a different information-carrying capacity.

Fibers are classified into two electromagnetic categories: single mode and multimode. The mode refers to the number of electromagnetic modes that exist in the fiber under certain conditions. Each electromagnetic mode in a fiber has its own unique electric and magnetic fields that are setup in the fiber. The mode also has a unique propagation constant. Single mode fiber allows for higher data-rates than multimode when operated under identical conditions.

Optical fiber can attenuate and distort the optical signal. The attenuation per unit length of high-quality fibers is shown in **Figure 3.9.** Notice that there are two minima located at 1.2 and at 1.55μm. Optical fiber can also distort the optical signal through dispersion, one example is pulse broadening: as the pulse travels down the fiber the pulse gets wider in the time domain. Single mode applications are typical more sensitive to signal attenuation and distortion than multimode applications. For a more detailed

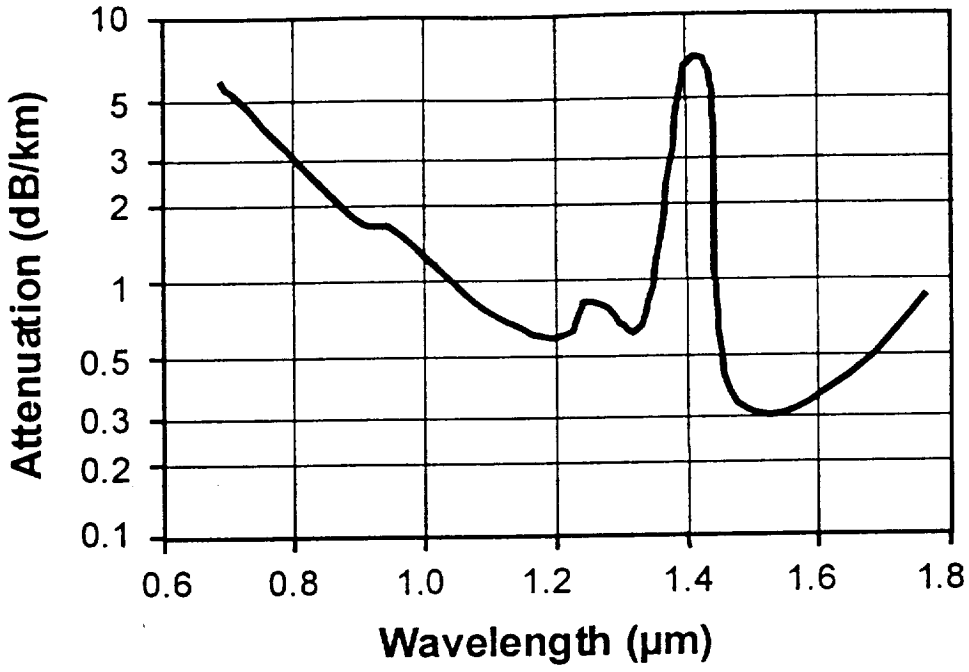


Figure 3.9. Fiber induced attenuation for various wavelengths. [After Miya-79]

discussion on optical fibers see most any text on fiber-optic communications, for example [Agrawal97].

### 3.2.3 Receivers

An optical receiver is a combination of an optical detector, amplifiers, and electronic processing elements used to recover the signal sent from the source. **Figure 3.10** gives a detailed block of a typical optical receiver [Agra-97]. The receiver is made up of three sections: 1) front end, 2) linear channel, and 3) data recovery. First is a discussion of the each section of the receiver is presented, then a brief description of photodetectors is given.

#### 3.2.3.1 Sections of a Receiver

The front end contains the photodetector and the preamplifier. The photodetector converts the optical signal to an electrical signal. This signal is very weak and therefore it must be amplified, the preamplifier amplifies the signal. A trade must be made between bandwidth and sensitivity of the photodetector-preamplifier pair [Agra-97]. A

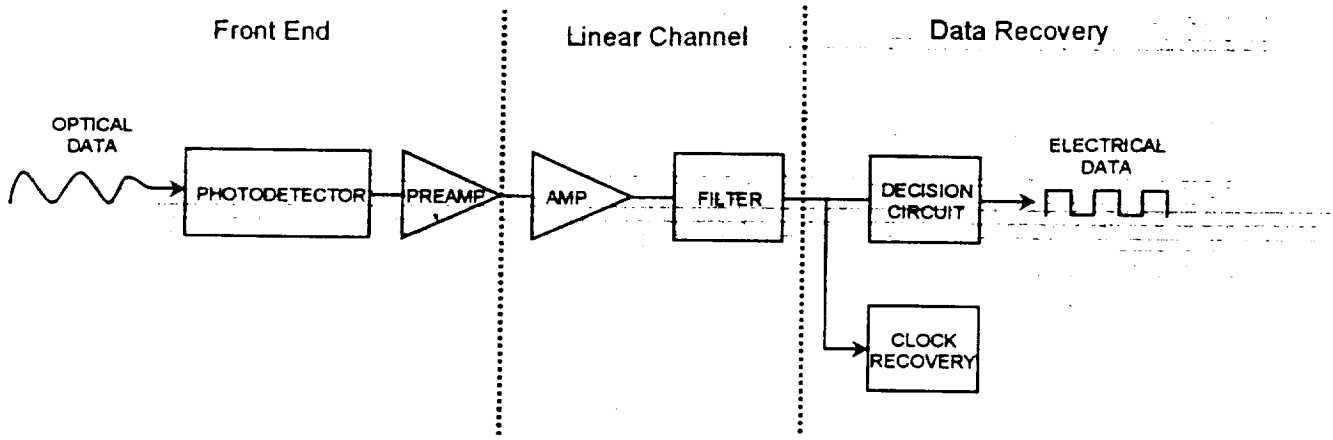


Figure 3.10 Block diagram of an optical receiver. The vertical dashed lines give the grouping of receiver components into three groups. (After Agra-97)

high resistive loading across the photodetector increases its sensitivity, however this loading also slows the response of the circuit. An equalizer is sometimes added to the circuit, it acts to attenuate the low-frequency components of the signal more the high-frequency components, in affect increasing the bandwidth of the circuit. Another method used to keep the bandwidth high while maintaining the desired sensitivity level is to use a transimpedance amplifier. Basically, in a transimpedance amplifier application the load resistor is placed as a feedback resistor around the preamplifier as opposed to a load across the photodetector, giving the amplifier more gain with little impact on circuit bandwidth. However, stability can be a significant factor when using transimpedance amplifiers.

The front end is followed by the linear channel. It consists of a high-gain amplifier and a low-pass filter. The amplifier boosts the electrical signal even more, sometimes using an automatic gain control that self-adjusts the gain based in the input signal. The desire here is to limit the average output voltage level regardless of average incident optical power. The low-pass filter shapes the voltage pulse and removes unwanted frequency components generated by signal processing.

The last section of the receiver is the data recovery portion. In this section of the receiver the clock and data are recovered. Transmitters can be designed to encode the clock signal into the data. The clock signal is regenerated using the clock recovery

circuitry. Another method of clock recovery is as simple as passing clock signal to the receiver.

The decision circuitry is used to recovery the data. It compares the output of the linear channel to a voltage reference called the threshold voltage. If the signal level is above the threshold then it is consider a "1", if not then it is a "0". The data sampling frequency and sampling duration is determined by the clock frequency. As will be seen later in this tutorial, the radiation sensitivity of the receiver depends strongly on the clock frequency, the sample window width, the delay between data edge and the decision window location within the bit period, and the relative location in the time domain of a radiation event.

### 3.2.3.2 Receiver Noise

The concept of determining a "1" from a "0" seems straightforward at first glance. But, the injection of noise into the receiver circuit causes some data bits to be interpreted incorrectly. Unfortunately, receiver circuits have inherent noise problems. At the frequency we are concerned with the two major mechanisms for inducing noise in a receiver are shot noise and thermal noise [Benn-60, MacD-62, and Robi-74].

Shot noise is a result of the random nature of electron generation. The incident optical power will generate a defined number of electron-hole pairs with a distribution of these carries in the time and space domain. The shot current is related to the variation in the probability of producing charge carriers over time and location. When considering shot noise one must include the effects from all components of the receiver [Agra-97].

Thermally generated noise is an intrinsic property of any conductor. Random thermal motion of electrons in some of the front end components of the optical receiver result in the largest current fluctuations. These current fluctuations are called thermal noise.

The total current is the sum of all current sources. Namely the current resulting from the optical power, the shot noise current, and the thermal noise current. The sum of these currents are interpreted as the data signal. If significant amount of noise exists, the data stream will have bit errors, incorrectly interpreted data. This will be revisited in Section 3.3.

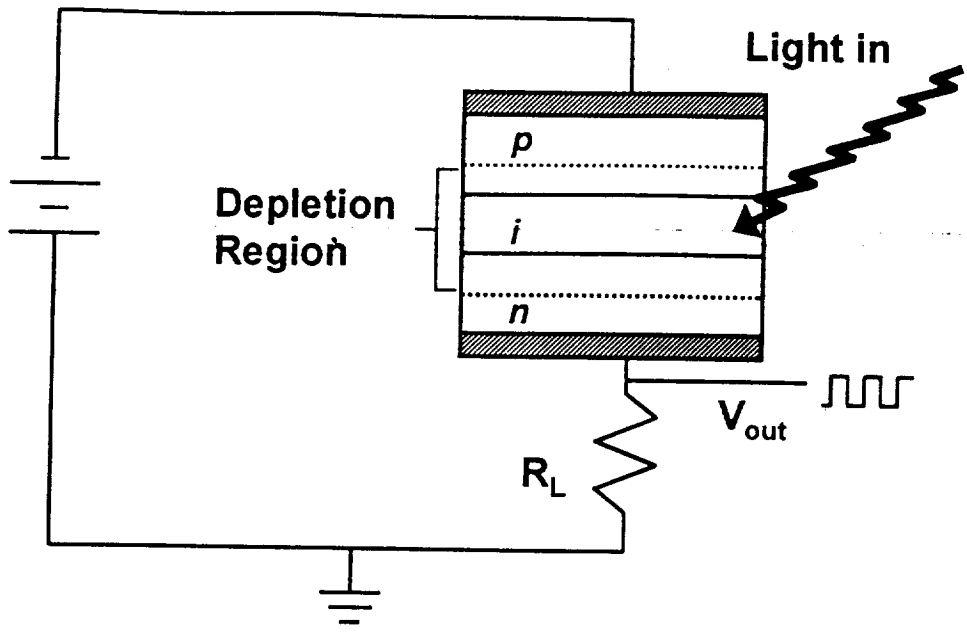


Figure 3.11 Schematic of a p-n photodiode. $R_L$ is the photodiode loading. The output level depends on the incident optical power

### 3.2.3.3 Photodiodes

This section presents a brief description of photodiodes. For more detail discussion on photodetectors see most any device physics textbook [Sze-98] or segment II of this short course.

Typically, if not always, photodiodes are chosen as the photodetector in high-speed fiber-optical data links. Three types of photodiodes used in fiber-optics are p-n photodiode, p-i-n photodiode, and avalanche photodiode (APD). The first and last are less likely to be used that the p-i-n diode.

The conversion of optical power into an electrical current can be understood by reviewing **Figure 3.11**. The p-n photodiode is operated in a reverse bias circuit. The incident light must penetrate to the depletion layer (a region in the diode that has a high electric field due to the applied voltage and the semiconductor doping concentrations). If the energy of the incident photons exceed the bandgap energy of the semiconductor ($E_g$), an electron-hole pair is created. The electric field in the depletion region drives the electrons towards the n-region and the holes towards the p-region. This current is the called photocurrent. It is proportional to the incident optical power. The logic output of a "1" or a "0" is determined by the incident optical power. The proportionality constant

of the ratio of the photocurrent to the incident optical power is called the responsivity. The responsivity is dependent on the photodiode material and the wavelength of the incident light.

A maximum cutoff wavelength can be determined based on the fact that the bandgap energy sets the limit on the creation of electron-hole pairs. That is, there is some value of the photon wavelength that if exceeded the semiconductor does not generate a photocurrent. This is given by:

$$\lambda_{max} = \frac{hc}{E_g} \qquad \text{(Eq. 3.5)}$$

where h and c are defined in Equation 3.2. **Table 3.2** lists some representative photodiode materials and their maximum wavelengths that can be detected. Most long-wavelength photodiodes are fabricated using Si, while short-wavelength applications use InGaAs.

Table 3.2 Cutoff wavelengths for various photodiode materials.

| Material | Wavelength (μm) |
|---|---|
| GaAs | 1.0 |
| Ge | 1.9 |
| InGaAs* | 1.7 to 1.1 |
| InP | 0.95 |
| Si | 1.13 |

*typical values depending on relative concentration

A p-i-n diode is fabricated with a large intrinsic semiconductor layer between the p and n-regions. This intrinsic layer acts to increase the depletion layer, giving a large region for photon absorption. Because of the high resistance of this intrinsic layer most of the voltage drop occurs across it, most of the charge that contributes to the signal is generated inside the intrinsic layer. The width of the intrinsic layer determines the how efficient the diode is at converting optical power to current, i.e. the responsivity depends on the intrinsic layer thickness. However, the response time of the photodiode increases with increasing intrinsic layer thickness.

Direct bandgap semiconductors like Si and Ge require much thicker intrinsic layers, typically on the order of 20-50 μm. The response times of these devices are > 200ps. In

contrast, using direct bandgap semiconductors like InGaAs the intrinsic layers can be much smaller (3-5 μm), these devices will have much faster response times (<50 ps).

A final note: The creation of electron-hole pairs in the photodiode by the space radiation environment can dominate the performance of a photodiode, and in-turn the data link performance. This topic will be explored in much more detail in the sections that follow.

### 3.2.4 Support Electronics

Most optical data links require a set of support electronics to format the data signal for optical communication. Some examples are buffering, encoding, decoding, voltage level shifting, digital data handing, temperature compensation circuitry, clock recovery circuitry (e.g., phase locked loops), and others. To impliment these functions links may contain MUX, deMUX, ASICs, RAMs, PROMs, protocol ICs, oscillators, and many combinations of the host of linear, digital and passive microelectronics and components available.

A discussion of these microelectronics (if the authors could be convinced to write this section) would cause the short course to be volumes thick. Therefore a detail discussion is beyond the scope. The reader should be warned that radiation effects in the support electronics can dominate the response of the data link, we will give some of the general concerns in Section 4.0.

## 3.3 System Performance Metrics

Optical data link operation can be degraded when exposed to a radiation environment. Certain performance metrics can be used to understand how link operation is degraded. Namely, power budget analysis and bit-error ratio (BER, sometimes called bit-error rate). In the sections that follow we will discuss each of these, but first we will look at a measurement technique called eye diagram which is a simple technique whose result is an easy-to-view approach at determining overall link performance.

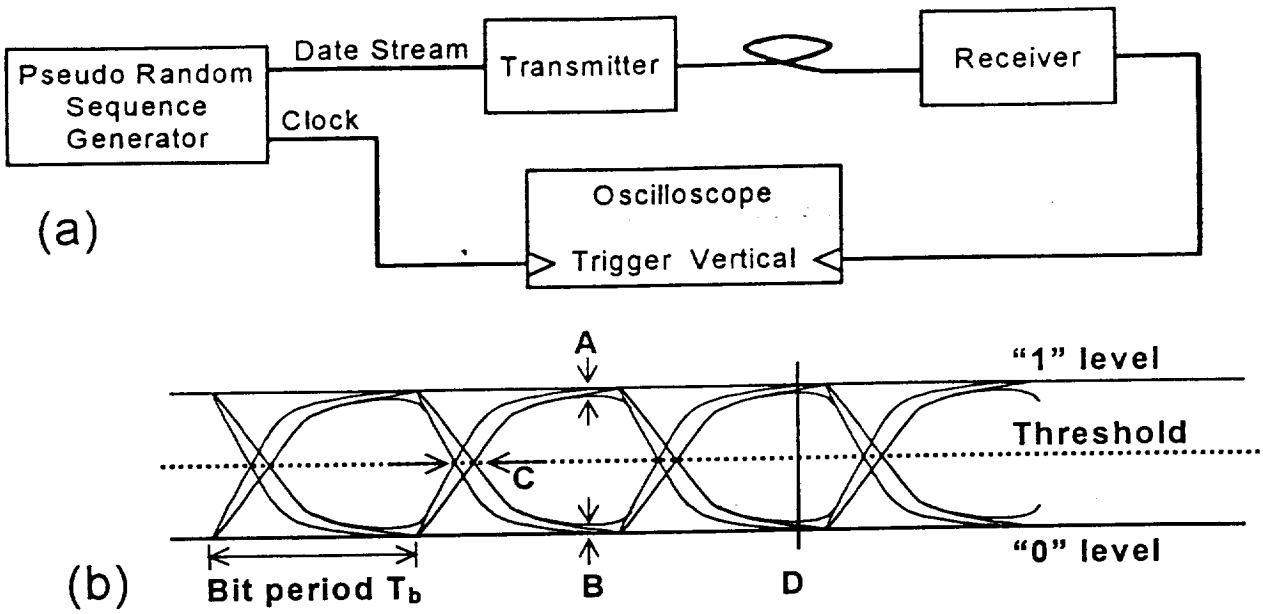


Figure 3.12 (a) Experimental setup used to measure an eye diagram. (b) Representation of an eye diagram.

### 3.3.1 Eye Diagram Measurements and Analysis

High-data-rate optical link performance can be measured using eye-diagram technique [Keis-91] (sometimes called eye-pattern). **Figure 3.12.A** shows a block diagram of the setup to make a time-domain measure of the bit stream. The pseudorandom sequence generator outputs a repeatable and predictable, but random data bit stream. The receiver output flows into the oscilloscope vertical trace, while the data clock activates the oscilloscope trigger. The result is a superposition of several bit sequences, an example is shown in **Figure 3.12.B**.

The eye diagram contains easily observable information about the overall link performance. Some of its characteristics are:

- The eye opening gives the optimum sampling time-interval for the received signal. The optimum sample time is where the eye is a maximum, e.g., the location labeled "D" in **Figure 3.12.B**.
- The voltage spacing labeled "A" is a measure of the noise when a logic "1" is transmitted, likewise "B" is a measure of the noise when a logic "0" is transmitted.
- The time spacing labeled "C" is a measure of the timing jitter. Jitter is a measure of the timing accuracy of the data stream.
- Increasing the frequency until the maximum operating frequency is reached will force the eye to close.

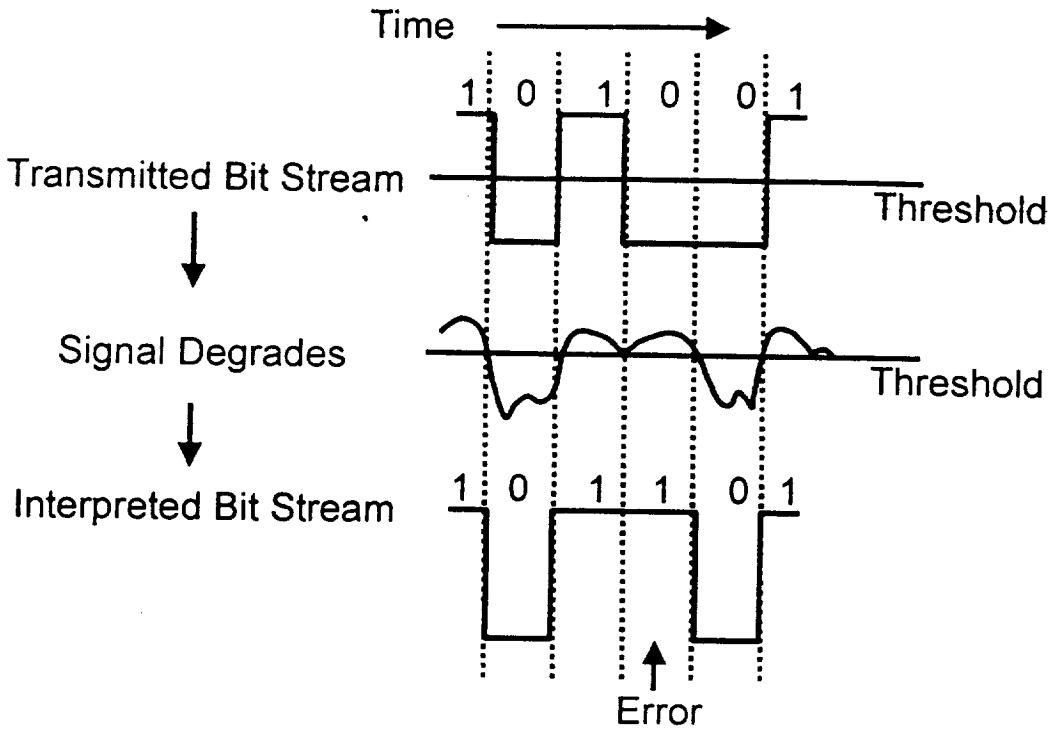


Figure 3.13. Cartoon of a bit sequence traveling through a data link. The fourth bit in the sequence is interpreted incorrectly.

### 3.3.2 Bit-Error Ratio

Data transfer by optical data links (or any data link for that matter) can be corrupted by system noise. These fluctuations in the data will cause data bits to be interpreted incorrectly. **Figure 3.13** is a cartoon of a bit sequence as it propagates through a data link. The top line shows the "ideal" input signal. The second line demonstrates a degraded signal after passing through the electronics and optoelectronics, the signal degradation may be a result of several sources of noise in the data path. The last line represents the received signal. Following the forth bit in the data sequence as it travels down the data path shows that in this case it was interpreted incorrectly. This is known as a bit error.

Depending on the operating frequency, several millions to billions of bits travel through a system every second, knowing the probability of incorrectly interpreting a bit is a useful metric. This probability is known as the bit error ratio (BER, or sometimes called the bit-error rate) and is given in Equation 3.6.

$$BER = \frac{\text{number of incorrectly transmitted bits}}{\text{total number of bits transmitted}} \qquad \text{(Eq. 3.6)}$$

This metric can be measured using bit error ratio test (BERT) equipment. Several companies sell this hardware. A general BERT setup will be described in Section 5.1.2.

The relationship between signal level, noise level and BER can be understood as simply as the more margin that exists in a system the less like a bit is to be in error. Decreasing the optical power launched on the photodiode lowers the BER.

### 3.3.2 Optical Power Budget

When designing an optical data link the designer must have a clear understanding of the power budget. There must be sufficient link margin to accommodate power losses as the data passes through the link. The starting point for this is the source output optical power, the end is point is the optical power that needs to be launched on the photodiode to achieve a certain BER. The choices associated with the optical source and photodetector must consider the power losses in the system and the required BER. Losses like:

- source-to-fiber coupling loss at the transmitter,
- connect insertion loss,
- fiber-to-receiver loss,
- aging effects, and
- fiber losses,

must be consider when characterizing the optical power budget for a link. **Figure 3.14**, represents a graphical analysis of the power budget for an optical data link. The link will transmit data with an acceptable BER as long as a fiber that is less than approximately 2.5 km. This type of analysis that includes radiation effects must be done for optical links used in the space radiation environment.

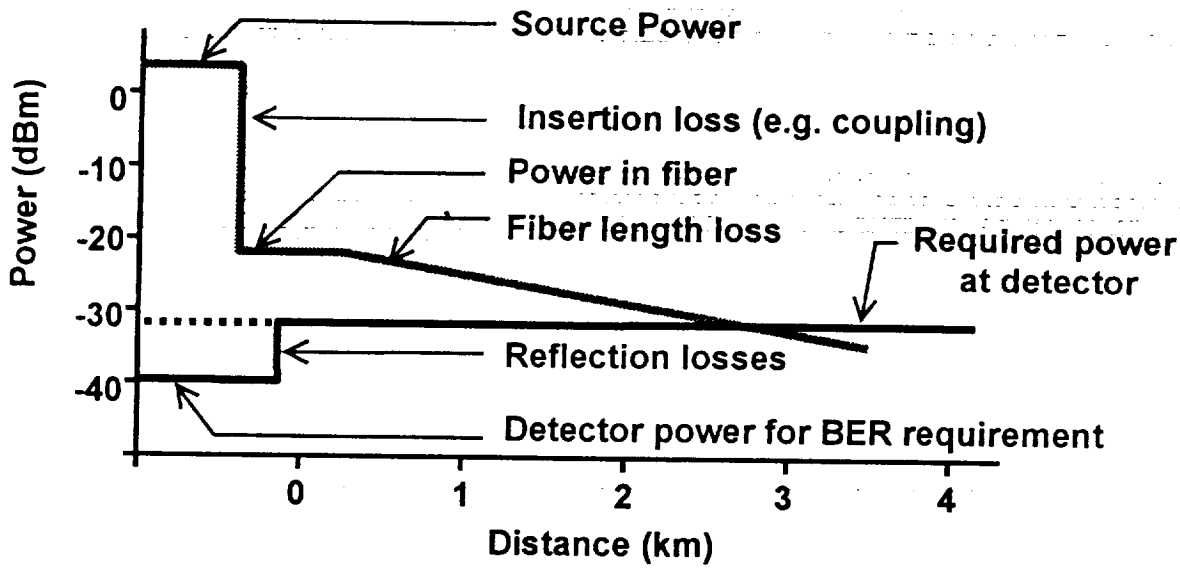


3.14. Graphical analysis of power budget.

## 4.0 Radiation Effects in Optical Components

The previous section gave an overview of the basic components of a Digital Optical Data Link, as well as discussing some of the metrics used to measure the performance of these systems. In this section, we will briefly consider the radiation effects to which these components may be susceptible and how these effects may degrade component performance.

We will first briefly consider DDD in light sources—LEDs and laser diodes. This subject will be treated in more detail in segment II of the short course. Next we will consider the effects of TID on the passive transmission media used in fiber-optic data links. We will then examine the effects of TID, DDD and single-event transients in photodetectors. Lastly, we will briefly discuss radiation effects in the support electronics.

### 4.1 Permanent Degradation of Sources

As mentioned in the previous section, the role of light sources in digital optical link systems—usually LEDs and laser diodes—is to convert current signals into light. Because the drive signals for these devices are usually on the order of milliamperes, the small currents generated by ionizing radiation (usually picoamperes) are insufficient to cause SEEs. As such, for these devices, we are generally more concerned with permanent degradation due to TID or DDD.

Both LEDs and laser diodes produce light by means radiative recombination of injected minority charge carriers with majority carriers in the depletion region. As such, any damage that decreases the efficiency of radiative recombination or introduces competing processes will degrade device performance. Irradiation by heavy particles such as protons and neutrons can displace nuclei from the crystalline lattice, causing DDD. These defects can serve as sites for nonradiative recombination, decreasing the efficiency of the light source. DDD effects will be covered in detail is Segment II of this short course. Here we merely note that displacement damage decreases the output power of these light sources, as well as increasing the threshold current for laser diodes (see **Figure 4.1**). We also note that with the exception of amphoterically doped LEDs, these

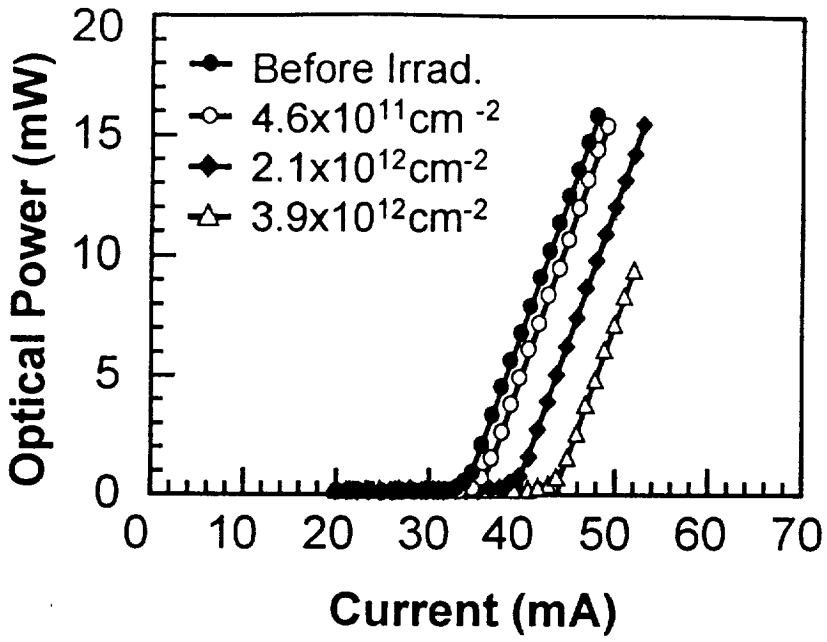


Figure 4.1 Displacement damage from proton irradiation increases laser diode's threshold currents and decreases their output power.

devices can remain functional even after exposure to relatively high proton fluences, provided the drive currents are sufficiently high to compensate for the effects of DDD.

Characterization of light sources continues to be an active area of research, with substantial effort directed toward the study of damage mechanisms and annealing in LEDs and multi-quantum well laser diodes. Indeed, many new optoelectronic technologies seem to show promise for future space missions.

It is interesting to note that even when one early study observed degradation in the radiation response in optoelectronic systems found loss of efficiency at relatively modest doses, the light source was vindicated upon further investigation [Mars-94b]. It turned out that the degradation actually took place in a graded index lens coupling the laser to the fiber, rather than in the laser diode, itself. This anecdote demonstrates not only that most light sources are remarkably hard to radiation, but that in contrast to the situation in microelectronics, in optoelecronics one cannot ignore radiation effects in the so-called passive media.

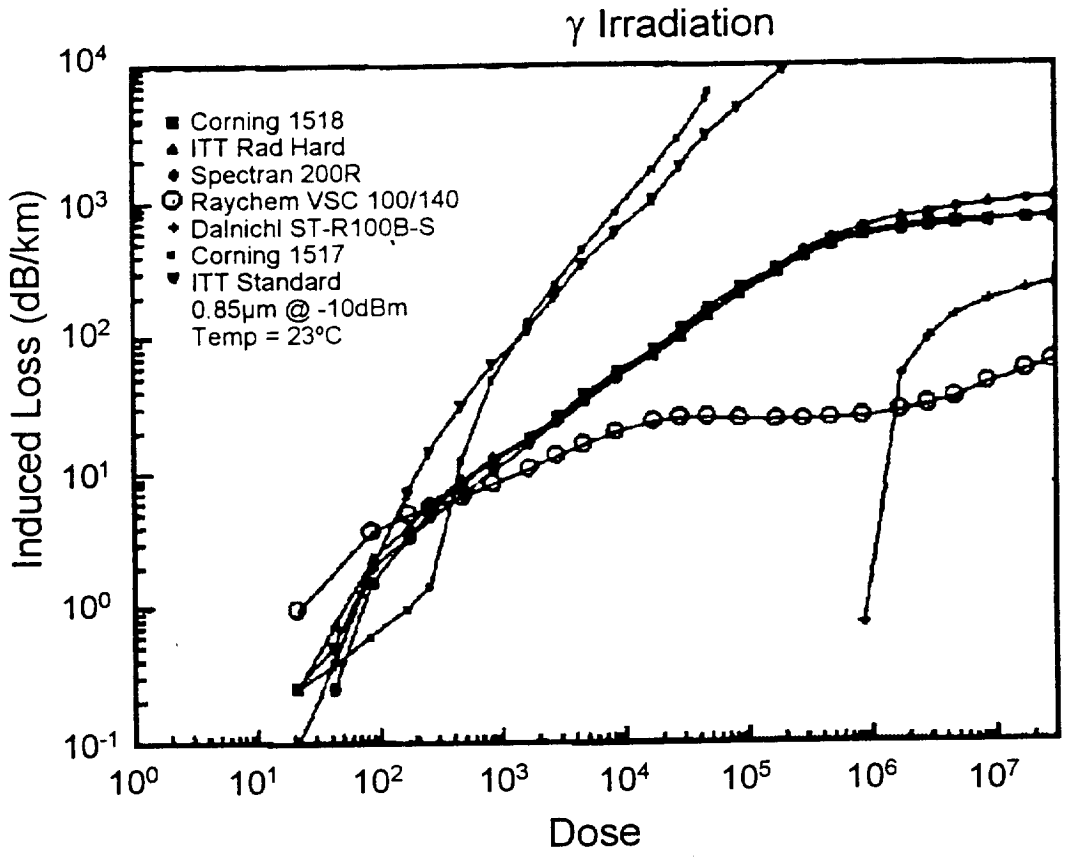


Figure 4.2 Phosphorus-doped, germanium-doped and pure-silica optical fibers can show quite different susceptibilities to proton-induced attenuation loss.

## 4.2 TID Degradation of Transmission Media

Although, charged particles traversing an optical medium can generate photons, these processes are too weak and the path lengths traversed to short for these events to interfere with signals. For this reason, with respect to transmission media, we are generally more concerned with permanent, cumulative degradation resulting from TID and DDD.

Photonic systems require nearly flawless optical fibers, lenses and other transmission media to transmit light over long distances with minimal losses. In what follows, we will concentrate on optical fibers, because they account for most of the pathlength traversed by the signal. It should be remembered that our treatment applies equally to lenses and other transmission media.

Ionizing radiation causes charge to become trapped by defects in the optical fiber, creating color centers that absorb electromagnetic radiation and decrease transmission efficiency. Because this effect can be important for some missions, we will treat it in some detail. Readers who require additional detail are referred to the 1991 short course given by E.J. Friebele [Frie-91]

As in microelectronics, the phenomenon responsible for TID induced performance degradation of optical fibers is charge trapping by defects in the material. These defects may be radiogenic themselves, or they may be the result of impurities or fabrication conditions. Regardless of the defect origin, once the color centers form, light transmission efficiency is degraded as the color centers absorb signal photons. The degradation, however, need not be permanent. As is the case for trapped charge in microelectronics, fiber optic color centers can heal by annealing. The processes of color center formation and annealing take place in competition, and the balance point for these processes determines the ultimate extent of fiber-optic degradation.

Even after two decades of study, not all of the processes involved in radiogenic degradation and annealing are completely understood. However, the factors that affect the radiation response of optical fibers are sufficiently understood that the designer now has a good basis for both fiber selection and for formulating a hardness-assurance test program. Among the most important factors that influence both radiation response and annealing are the properties of the fiber itself, the temperature and optical conditions encountered in the application and the radiation environment to which the fiber is exposed.

A quick glance at **Figure 4.2** is sufficient to indicate that radiation response of various optical fibers can vary widely. Attenuations after the relatively modest dose of 1 krad(Si) range from undetectable to around 100 dB/km. The annealing behavior of different fibers is every bit as variable. Much of the variation can be accounted for by the properties of the fibers themselves. Among the more important fiber properties that affect radiation response is fiber composition. As seen in **Figure 4.2**, pure silica fibers are less susceptible to radiation damage than are those with more complex compositions. However, optical fibers are usually fabricated with dopants tailor refractive indices of the fiber core and clad to the desired application. Both germanium and phosphorus are

commonly added to the core to raise its refractive index, while fluorine is used to lower the clad refractive index. Dopant choice can have important consequences for radiation hardness. In general, phosphorus seems to facilitate the formation of color centers that attenuate light signals, while germanium actually seems to improve some aspects of radiation performance. As might be expected, manufacturing conditions can also influence radiation and annealing response. The manner in which the fiber preform is deposited and under which the fiber is drawn are among the conditions found to correlate with radiation response.

The conditions encountered during the application can also influence requirements for the radiation performance of passive optical components. Annealing in optical media—as in microelectronics—is a thermally activated process. In one study, [Frie-91] fits to activation energies for various color-center traps have yielded activation energies on the order of 1 eV, or so, and trap lifetimes ranging from about a thousand to a few tens of thousands of seconds at room temperature. Moreover, studies have shown that the annealing rate of phosphorus-doped fibers does not increase with temperature. As such the temperature range encountered in the application can influence fiber choice as well as testing procedures.

Radiation damage can also be annealed by the light signal itself. This process, called photobleaching, occurs when the light supplies enough energy to facilitate annealing in the fiberoptic. Even very modest signals can significantly alter the equilibrium between damage and annealing. In space, radiation damage and annealing take place as competing processes, with temperature and signal intensity playing crucial roles in determining the equilibrium point.

One of the most important application conditions in determining how badly radiation undermines system performance is the signal wavelength. Most color centers have their peak absorption in the ultraviolet. The further away the source wavelength is from the absorption peak, the less will the signal be absorbed. This provides some motivation for selecting systems that use InGaAsP laser diodes operating at 1300 nm over those operating at shorter wavelengths.

The radiation environment must also be considered when evaluating potential degradation of transmission media. For applications where the transmission length is

short, and where the light source can be driven hard enough to provide sufficient end-of-life margin, radiation-induced darkening of transmission media may be negligible for radiation levels less than $10^5$ rad(Si).

The dose rate and the type of radiation also affect the extent of radiation damage. The annealing and photobleaching that compete with radiation damage give rise to an apparent dose-rate effect. To date, however, there is little evidence for true dose rate dependence in optical media, and most studies show good agreement between low-dose rate data and higher-rate tests followed by an anneal. This means that a shorter, high rate test coupled with annealing data may suffice to predict radiation behavior in the low-dose-rate, on-orbit environment. Note, however, that some studies have shown enhanced susceptibility to radiation damage of Ge doped fibers for pulsed radiation sources.

The space radiation environment may include a broad range of radiation types. Because it is not practical to provide such a radiation mixture in the lab, most radiation test sources provide only one type of radiation (for example, 1.25 MeV $\gamma$ rays from $Co^{60}$). Several studies have sought to show that, at the very least, such a simplification will not significantly underestimate radiation damage. To date, most studies have shown that equivalent absorbed doses of gamma rays actually induce slightly more damage than an equivalent dose or protons or electrons. As such, one can make that conservative assumption that to first order, a rad is a rad, and data obtained with gamma rays can be used to bound the on-orbit behavior of the fiber. It should be noted, however, that different types of radiation might have different damage mechanisms. For example, protons, in addition to generating color centers, may also be captured within the medium forming SiOH, which absorbs strongly in the infrared. Care must always be taken when using data taken under different conditions.

The preceding discussion is intended primarily to give a reader an indication of the broad variety of factors that affect the radiation performance of optical fibers. For a deeper discussion of these factors, the reader is referred to reference [Mars-94b] and the references contained therein. For most applications, the reader will find that research done to date will be adequate to aid in selection of appropriate candidate fiberoptics and in developing hardness assurance test procedures for these candidates. The research

undertaken to date also suggests methods of compensating for radiation effects in optical media.

In addition to using spacecraft structures as shielding to minimize radiation exposure, there are a number of techniques for minimizing the effects of radiation damage in optical media. Selecting an optical fiber with known and appropriate radiation response for the mission environment is a first step. It should also be remembered that radiation damage takes place in competition with thermally induced annealing and photobleaching. In most applications, the equilibrium level of radiation damage will be lower if the optical fibers are kept at a higher temperature. (Note that phosphorus-doped fiberoptics are an exception.) Moreover, overdriving the light source, if feasible, not only facilitates photobleaching, but also can compensate for any attenuation that takes place over time. Properly understanding the processes that contribute to darkening in optical media will ensure that these media are not the weak links in the optoelectronic system. Indeed, because of the role the detector plays in the data link system, this device is more likely to be the weak link.

## 4.3 Permanent Damage in Optical Detectors

The purpose of the detector in an optical system is to detect a weak optical signal and convert it into an electrical current that can then be amplified sufficiently to allow the resolution of individual data bits. Each of these steps—detection, conversion and amplification—is potentially vulnerable to radiation effects. Here we consider the effects of TID and DDD on the most common optical detectors, while in the next section we will examine the potentially significant role of single-event transients in these devices. It will be seen that radiation characteristics play an important role in determining which detectors are suitable for space applications.

Optical detectors in optoelectronic devices function by detecting the photocurrent generated by a photon with energy greater than the semiconductor band gap. For this reason, any damage to the semiconductor that changes its global properties, or that degrades the semiconductor's ability to carry a current will potentially compromise the detector's efficiency. Because DDD generates charge traps that significantly decrease

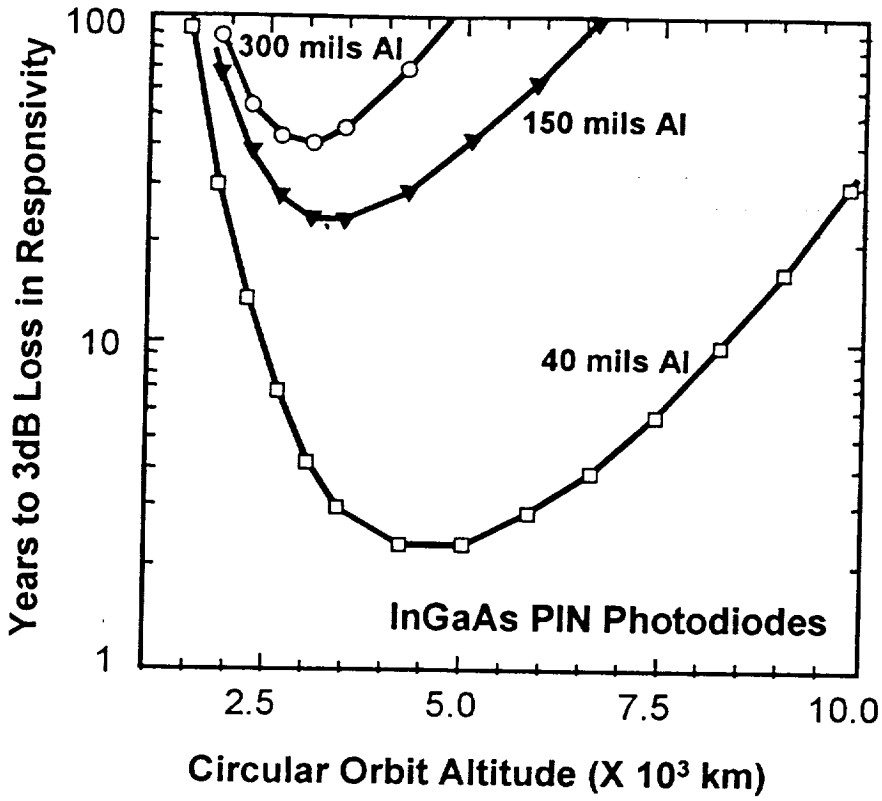


Figure 4.3 Equivalent Al shielding thickness can have a large effect in determining how long a photodetector may operate before the environment inflicts a particular damage level.

minority carrier lifetime, minority-carrier photodetectors—such as phototransistors—are generally unsuitable in high-radiation environments. This is a prime reason why photodiodes predominate in high-radiation applications.

As TID accumulates, photodiodes, like all diodes, degrade, with leakage currents increasing up to several orders of magnitude for doses up to 1 Mrad(Si). Both TID and DDD increase background noise in photodiodes, and DDD tends to decrease receiver current outputs. However, many photodetectors show remarkable robustness to space radiation environments. **Figure 4.3** shows the number of years a typical InGaAs PIN photodiode would take to suffer a 3 dB responsivity loss for various equatorial circular orbits and behind various shielding thicknesses. Often the key to success is incorporating adequate margin in source strength to account for EOL degradation in detectors. In most

cases, the photodetector will prove to be more robust as far as TID and DDD are concerned than will many electronic components. Session II discusses DDD in photodetectors in more detail

### 4.3.2 Single-Event Transients in Photodetectors

As outlined previously, photodetectors detect light signals by means of the photocurrents they generate in the semiconductor. However, these photocurrents can be indistinguishable from the single-event transients (SETs) generated by ionizing radiation. For this reason, SETs can combine with other sources of noise (particularly near EOL) to significantly increase the bit-error ratio in high-radiation environments.

Fortunately, the SEE susceptibilities of many photodetectors have already been characterized, and this work can be used to guide detector selection for high-radiation environments. Some devices are very susceptible to SETs, while others seem to be virtually immune to them. Indeed, recent work demonstrates that some detectors are even susceptible to proton-induced SETs caused by direct ionization.

As discussed in section 2, protons can generate ionization by either direct means—in which the proton, itself generates the charge—or by indirect means—in which the products of a proton-nucleus collision generate the charge. If sufficient charge is generated and collected at a sensitive node in an electronic device, an SET or an SEU may result, see **Figure 4.4**. For most microelectronics, proton direct ionization is far too feeble to be an SEE concern. The high sensitivity of photodiodes, however, means that even proton direct ionization cannot be ignored by the SEU analyst.

**Figure 4.5** demonstrates this rather surprising result. As can be seen, the SET cross section for protons at near-grazing incidence is more than an order of magnitude higher than the cross section for normally incident protons—this despite the fact that the physical device cross section is actually lower for grazing-incidence protons. This result has been interpreted as an indication that for sufficiently long path lengths within the detector, even protons can directly generate enough ionization to cause SETs. Further support for this interpretation is given by comparing results for low-energy protons with those for protons of higher energy, see **Figure 4.6.** Because LET decreases with proton

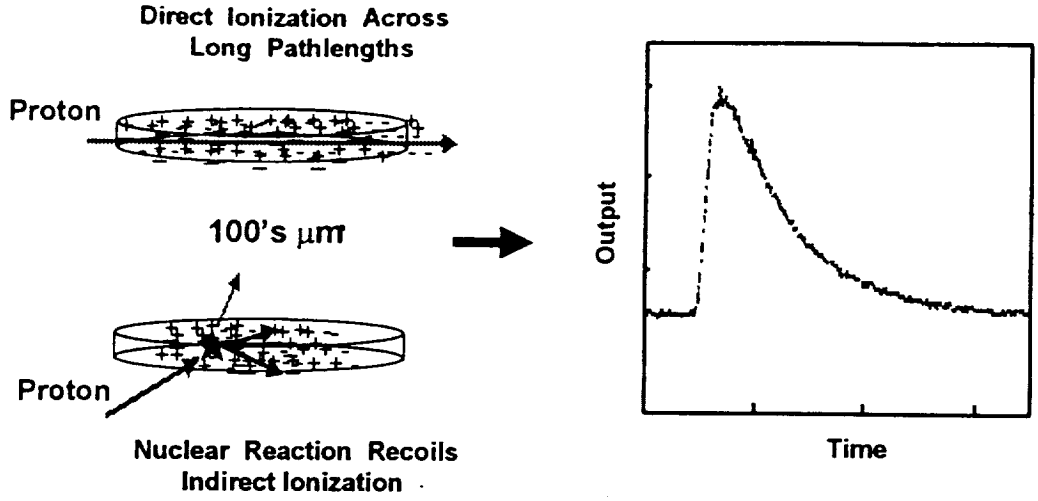


Figure 4.4 Protons can generate charge in a device by either direct or indirect ionization. If sufficient ionization is generated, a single-event transient (SET) may result.

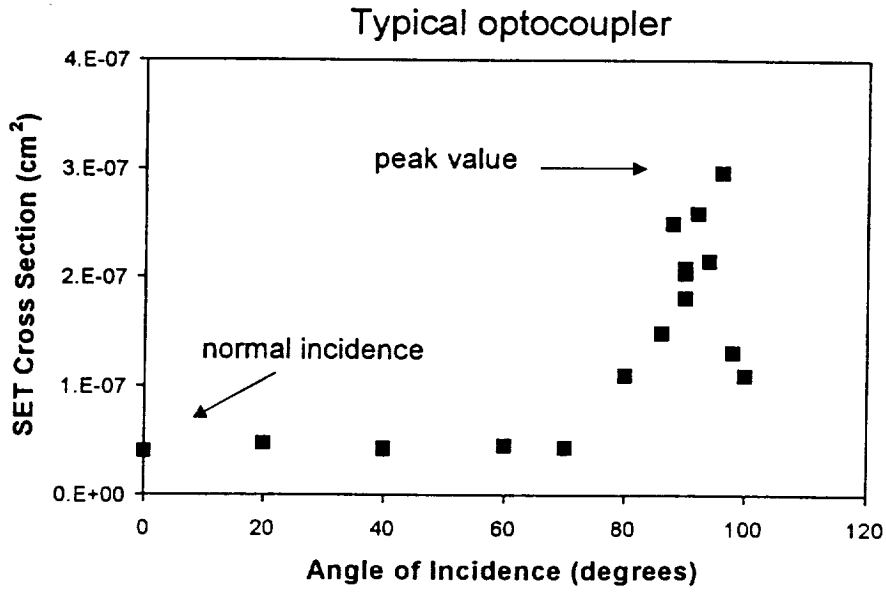


Figure 4.5 The SET cross section for protons incident on a photodiode increases dramatically as the protons approach grazing incidence—an indication that direct ionization is becoming important.

energy (over the energy range of interest), direct-ionization would be expected to be less important for higher-energy particles. Indeed, no enhancement is seen at glancing incidence for 225 MeV protons, while substantial enhancement is seen at near-grazing incidence for 68, 40 and 30 MeV protons. A consequence of the increase in grazing-

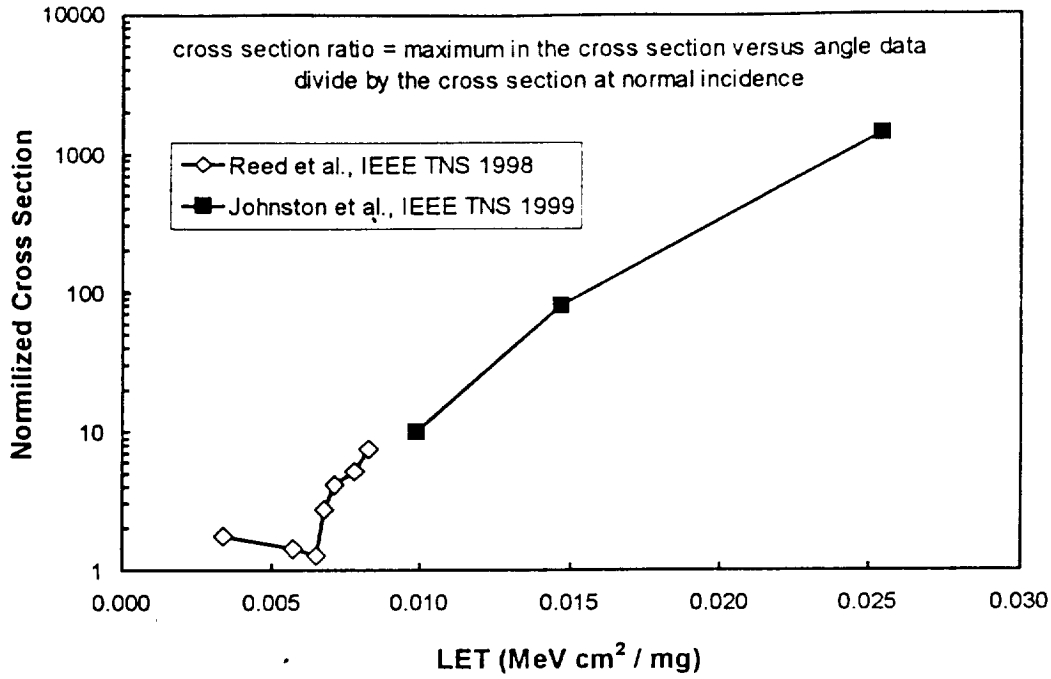


Figure 4.6 More proof of direct-proton-ionization SETs comes from proton experiments at different energies. Protons with higher energies (68-225 MeV) and therefore low LETs, have low cross sections, while for low-energy (15, 30 and 50 MeV) protons, which have higher LETs, the cross section increases dramatically.

angle cross section is that in proton-rich environments, proton-induced SETs can dominate those caused by heavier ions and by indirect ionization.

The susceptibility of photodetectors to direct-ionizing proton SETs demonstrates the importance of minimizing the volume in which the detectors are susceptible to ion-generated photocurrents. This criterion can be extremely important in selecting components that may perform acceptably in space radiation environments. As was discussed in Section 3 of this short course, direct-bandgap semiconductors, such as GaAs and InGaAs, require much thinner intrinsic semiconductor layers than do indirect-bandgap semiconductors, such as Si and Ge. As a result, not only are direct-bandgap devices more suitable to high-data-rate applications, they are also less likely to generate large, ion-induced photocurrents, and so are less susceptible to SETs.

However, knowing the device SET rate is only one step in determining how these events will affect system performance metrics such as the bit-error ratio (BER). As is the case with most SETs, system-level characteristics are crucial for understanding whether

SETs will affect system performance. System-level aspects of SET assessment for fiber-optic data links will be discussed in more detail in Section 5. Here we merely note that it is system-level characteristics that determine whether an SET of a given size and duration will cause a bit error. Because of the periodic nature of the signal, whether an SET causes a bit error depends critically on both its magnitude and on when it occurs with respect to when the signal is read. As such, high-rate applications will be more susceptible to SETs than will slower applications. Moreover, because receivers typically set the threshold for discrimination between '0' and '1' midway between the lowest and highest optical powers, increasing the source intensity significantly lowers the number of SETs that ultimately contribute to the BER. Note that with respect to detector SETs, as with respect to TID and DDD induced degradation in sources, transmission media and detectors, extra margin in light source drive can significantly improve system performance.

### 4.5 Radiation Effects in Support Circuitry

As indicated in Section 3, the receiver must not only detect a weak light signal and convert it into a current, but also amplify it and then process it. The photodiode can only accomplish the first two of these processes. Amplification and processing require additional support electronics. The devices that perform these functions are inherently vulnerable to the same radiation effects that plague all electronics. In many cases, one may devote considerable care to selection of appropriate light sources, transmission media and detectors only to find the most vulnerable component in the system is, for example, an op amp or an A-to-D converter.

In particular, for a fiber-optic data link, two of the most vulnerable phases of data processing are the amplification stage and the discrimination stage—that is, the stage where the system decides where a bit is a '0' or a '1'. The amplification stage can introduce transients of its own, in addition to amplifying noise from upstream. The discrimination process involves comparing the signal to a reference signal, and, this too can introduce errors.

Perhaps a more significant worry arises from the high data rates of FODLs. In general, such high data rates require state-of-the-art, high-speed electronics to avoid being overwhelmed. It is important that such components be characterized for susceptibility to TID and DDD induced degradation, and especially for single-event induced hard failures. Moreover, the same concerns apply to the electronic portions of the data link as apply to the optoelectronic portion: In many applications, the bit-error ratio is proportional to the data rate.

Overall, the components in fiber-optic data links can perform well in high radiation environments. However, ensuring such performance is a matter of following good hardness assurance practices for both optical and electronic portions of the system from the component level to the system level.

## 5.0 Optical System Response to Space Radiation Environments

This section discusses radiation effects issues related to optical data link system performance in the space radiation environment. The goal is to help the reader gain a better understand of how the component level radiation effects (Section 4.0) affect the link performance metrics (Section 3.0). System level single event effects ground testing is discussed, followed by system level performance metric analysis including radiation effects on selected components, finally we present some on-orbit results of a few fiber link systems.

The optical data link system can contain a host of microelectronic and optoelectronic devices as well as passive optical components. Each of these devices can suffer performance degradation when exposed to the space radiation environment. It is beyond the scope of this course to cover every detail of optical link performance degradation due to all possible devices. Using good engineering practices in selecting and assessing the radiation performance of these device will ensure that their impact on system performance will be minimized, several papers and short courses have been published on these topics [Kinn-98 and LaBe-96]. Component level TID, displacement damage and some SEE screening is typically sufficient to assess the performance of most microelectronic and photonic devices in the space radiation environment. There are exceptions to this, for example SEU characterization of microelectronic devices that induce bit errors in the data stream.

This section of the short course will cover system impacts when optical and optoelectronic devices experience performance degradation when exposed to radiation. These devices include optical sources, optical fiber, and photodetectors. Some of the testing techniques and analysis are general, we attempted to indicate when a technique or analysis approach can be used to assess other component effects.

### 5.1 System Level Single Event Effects Ground Testing

This section summarizes the impact of single ionizing particle events on optical links operating in the MHz to GHz regime. First we will describe radiation induced bit errors, focusing on radiation events in photodiodes. Then we will describe the implementation

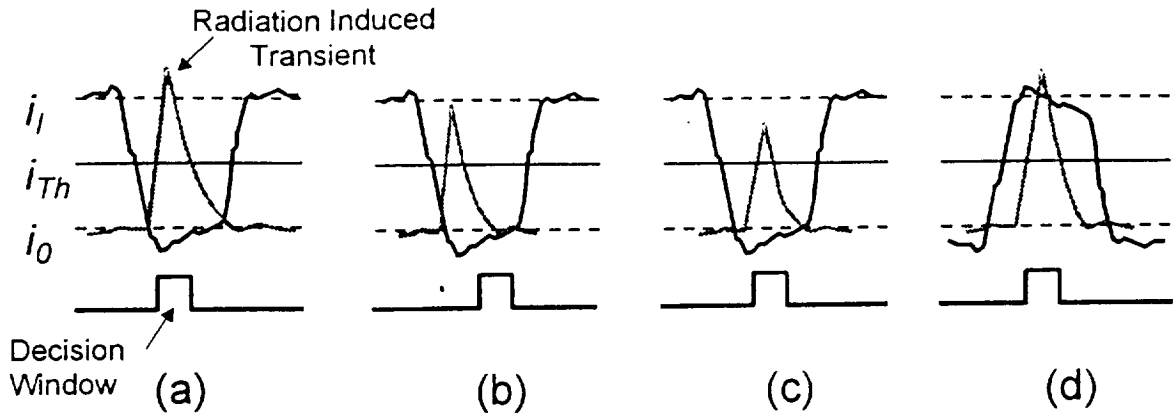


Figure 5.1. Particle-induced SETs occurring at different locations within a bit period and with different intensities [after Mars-96]. The event in (a) will cause a bit error, while those depicted in (b, c, and d) will not.

of and results from a generic BER test on a photodiode when exposed to protons and helium ions. One example of system level testing of a full functional optical data link is given, followed by a summary of results from *in situ* experiments on several other full-functional fiber-optic data buses.

### 5.1.1 Radiation Induced Bit Errors

As was shown in Section 3.3, noise can induce bit errors in the data stream. Likewise, single particle radiation events can also induce bit errors in the data sequence [LaBe-93, Mars-94b, Mesh-94, Mars-93b, Mars-94a, Dale-96]. These single particle events can occur in any of the digital or linear devices in the data path. Photodiodes are particularly sensitive to ionizing radiation (the basic mechanisms for these events were described in Section 4.3.2). Those used in optical links typically have large junctions, fast time constants, and can detect a wide range of optical powers [Agra-97, Pala-98, DeCu-98, and Lach-98], photodiodes make perfect ionizing particle detectors.

The next few paragraphs will examine the particular case of how a radiation-induced current transient in a photodiode is detected by the decision circuitry of an optical data link and forms a bit error. We focus on photodiodes because of their specific use in optical data links and the likelihood of a radiation-induced event occurring within them. Keep in mind that any device in the data path can cause bit errors.

Studies on several high-speed digital optical links have shown that photodiodes can be the most sensitive component to single particle events [Fritz-95, Mesh-94, Mars-93b,

Mars-94a]. Energetic products from nuclear interactions between protons and semiconductor nuclei that traverse the photodiode can cause a data bit errors. Likewise, bit errors can result from heavy ion cosmic rays that traverse the photodiode. **Figure 5.1** depicts the affect of four different particle events on a data bit. **Figure 5.1.A** contains a sketch of a "0" level data bit that is part of a NRZ data stream (dark line). Superimposed on this sketch is the current pulse expected when an ionizing particle interacts with the photodiode (light line). In this case, the radiation event occurs during the decision time-window and with sufficient current to induce a bit error. The current transient depicted in **Figure 5.1.B** does not cause a bit error. The error has sufficient height, but does not occur within the decision time-window. The transient depicted in **Figure 5.1.C** may or may not cause a bit error. It occurs at a time that is within the decision window, but the induced-current level falls in a region that will be ambiguously interpreted by the decision circuitry. The current transient depicted in **Figure 5.1.D** does not cause a bit error, inducing more current when interpreting a level "1" does not affect the decision made by the decision circuitry.

From the interpretation of radiation-induced bit errors, we see that there is a finite probability of a "0" level bit transitioning to a "1" level when the photodiode is exposed to the space radiation environment. The System BER calculations must include bit errors caused by radiation events in the photodetector. And more generally, this is true for any device that are in the data path and is susceptible to radiation-induced bit-errors.

Bit errors that occur in any device in the data path are somewhat analogous to logic errors in memory devices, commonly known as single event upsets (SEUs). The main difference is that the cross-section for memory bit errors has a physical geometry associated with it. But, the cross-section for a bit error that occurs in a clocked bit sequence is associated with not only a physical geometry, but also a sensitive time window. The event must occur at a certain physical location, and it must occur within the decision window [Mars-94a, Reed96].

### 5.1.2 Radiation-Induced Bit Error Ratio Testing

It is desirable to collect bit error information in real time. That is detect, count and display the BER of an optical link as data is transmitted and detected by the link. A Bit

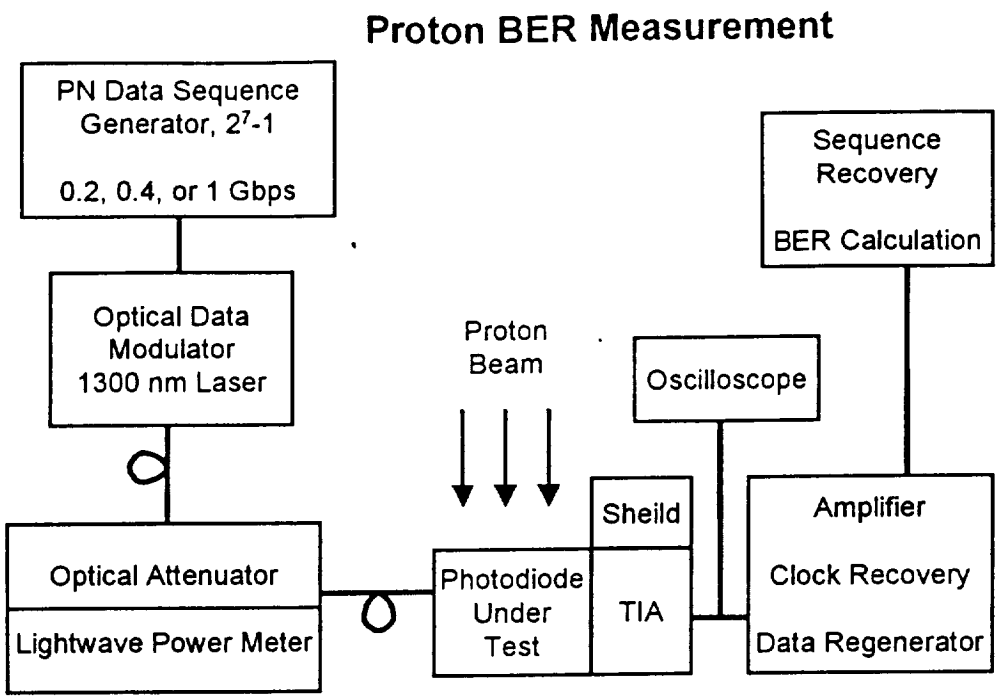


Figure 5.2. Block diagram of BER Test set-up.

Error Ratio Test (BERT) is one method of detecting bit errors in a clocked data sequence. At a minimum, a BERT determines the BER of an optical data link and/or the number of errors in a defined time interval (a specific test set may have other formats for displaying the data collected). For radiation characterization, we are interested in the number of errors that occur during a radiation exposure. These types of measurements are used to determine the error cross section when exposing a specific component of an optical data link.

In this section we will first describe how a BERT is used to determine the radiation sensitivity of a photodiode. Even though the discussion focuses on radiation events in photodiodes, some of the testing techniques are general and can be applied to other microelectronic and photonic components.

### 5.1.2.1 Proton-Induced SETs in Photodiodes That Cause Bit Errors

In this section we describe the use of a Broadband Communications Products, Inc. BERT to understand the mechanisms and effects of proton-induced single event transients photodiode (PD) as used in an optical data link. Keep in mind that some of the

test techniques are general and can be used to evaluate the radiation performance of many components of a optical data link.

The experimental setup [Mars-99, Mars-96, and Mars-94] is shown in **Figure 5.2**. The instrument control and data logging was done using customized software over GPIB interface. The data stream is generated by pseudorandom number (PRN) sequence generator portion of the BERT, the bit stream length was $(2^7-1)$. A waveform generator (not shown) operating at 200, 400 and 1000 Mbps supplied the clock signal. The optical attenuator regulates the power launched on photodiode. The light could be launch onto the photodiode via an optical fiber, or the fiber could be inserted into the lightwave meter so that the launched optical power could be measured. A 3D micro-manipulator stage is used to alignment of the optical fiber with the photodiode, an oscilloscope was used to monitor photodiode output to maximize coupling efficiency between the fiber and the photodiode. The photodiode used in these tests was a Epitaxx ETX 75 p-i-n ($In_{0.53}Ga_{0.29}As$). All circuitry outside the photodiode was shielded from proton irradiation, including the transimpedance amplifier. The BERT performed clock and data recovery, calculated and reported BER, reported the number of errors that occurred during an exposure and the percent of error free intervals. The percent of error free intervals helps to verify that each proton event cause one bit error. A BER of $10^{-9}$ was measured when the test set was sitting on the bench top, unexposed to any radiation environment. This is acceptable BER to ensure that the system will be free from errors induced by system noise during the time that it takes to make an irradiation.

Proton exposures, at 63 MeV, were carried out at Crocker Nuclear Laboratory, University of California [Mars-99, Mars-96, and Mars-94]. A single exposure, where at least 100 errors occurred, took a few minutes. After a proton exposure the BER, number of errors, percent of error free intervals, and proton fluence are recorded (recall that the error cross-section is found from the ratio of the number of errors to the proton fluence).

First, let's consider the bit error cross-section dependence on optical power, see **Figure 5.3** [Dale-96, Mars-96, and Mars-94]. Here we plot the cross-section at various optical powers when operating the link at 400 Mbps, the proton angle of incidence was 80 degrees. Notice that there are several orders of magnitude variation in cross section over optical power. An increase optical power launched on the detector causes an

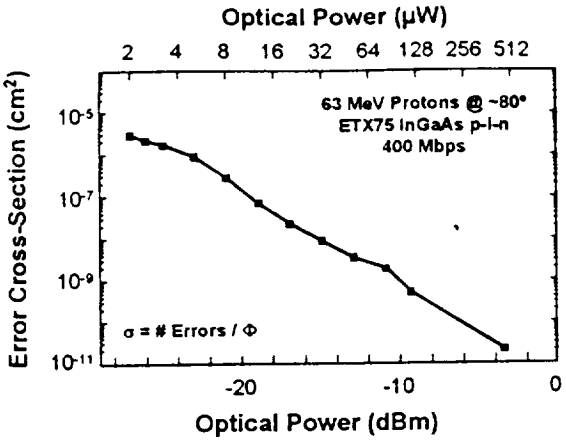


Figure 5.3. Variation of photodiode error cross-section over optical power.

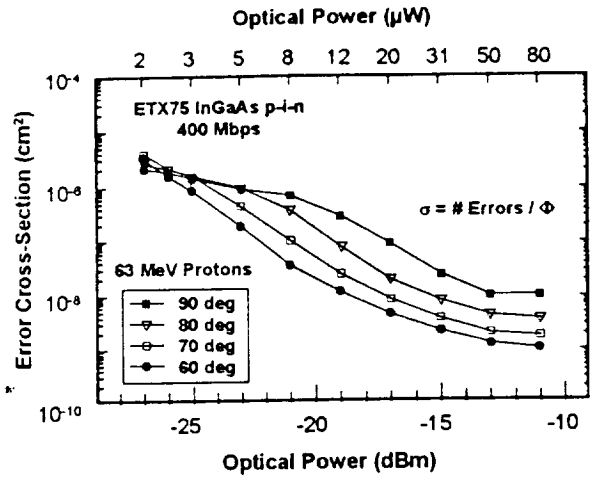


Figure 5.4. Proton-induced bit error cross section for various optical powers and angles of incidence

increases decision level. The photodiode is less sensitive to proton-induced events that result in low current levels, i.e. fewer protons cause an effect. An important consideration is that network topology affects optical power launch on the photodiode, e.g. star couplers. Characterization of bit error cross-section must accommodate the full range of the system optical power.

Next, let's consider the cross-section dependence on proton angle of incidence and the optical power. **Figure 5.4** gives the results of measurements made on the proton-induced bit error cross-section for various optical powers at four angles of incidence [Mars-96, Mars-94]. The angles are referenced to a line normal to the surface of the photodiode. These data demonstrate the fact that some of the proton-induced events are due to direct ionization, (as was for the photodetectors contained in optocouplers, see Section 4.3.2). Observing a few facts about the data uncovers the proton-induced direct ionization effects. Notice that there is a sharp increase in cross-section with angle of incidence at high optical power. This is inconsistent with solely indirect ionization events as the cause for bit errors. There is a possibility that the cross-section is some combination of direct and indirect ionization effects. Also, notice that at low optical power there is no change in the cross-section over angle of incidence. Correcting these cross-sections for angle of incidence shows that the cross-sections are near the geometric area of the photodiode. At this point the optical power is so low that very low levels of

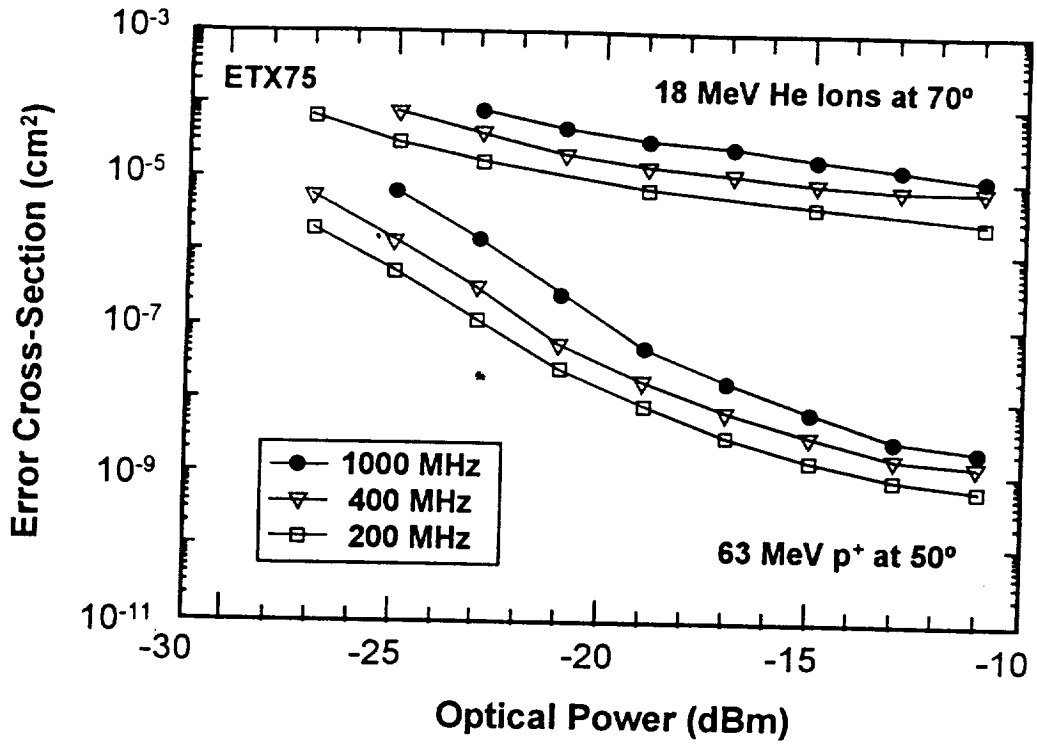


Figure 5.5 Frequency dependence of error cross section for various ions.

ionization will induce a bit error. There is more on this topic in Section 5.2.2 where we discuss on-orbit BER calculations.

Finally, consider **Figure 5.5** which shows the photodiode error cross-section dependence on operating frequency [Mars-99, Mars-96, and Mars-94]. Notice that at all optical powers for both protons and He ions the error cross section is linearly dependent on data rate.

### 5.1.3 System Level Radiation Effects Testing

In order to fully qualify an optical link for use in the space radiation environment several issues must be addressed. Some of these can be address at the component level, while others are quantified at the system or quasi-system level. Section 2.2 gives an overview of the issues that must be addressed. The list below gives an overview of how some of these effects affect device performance in general.

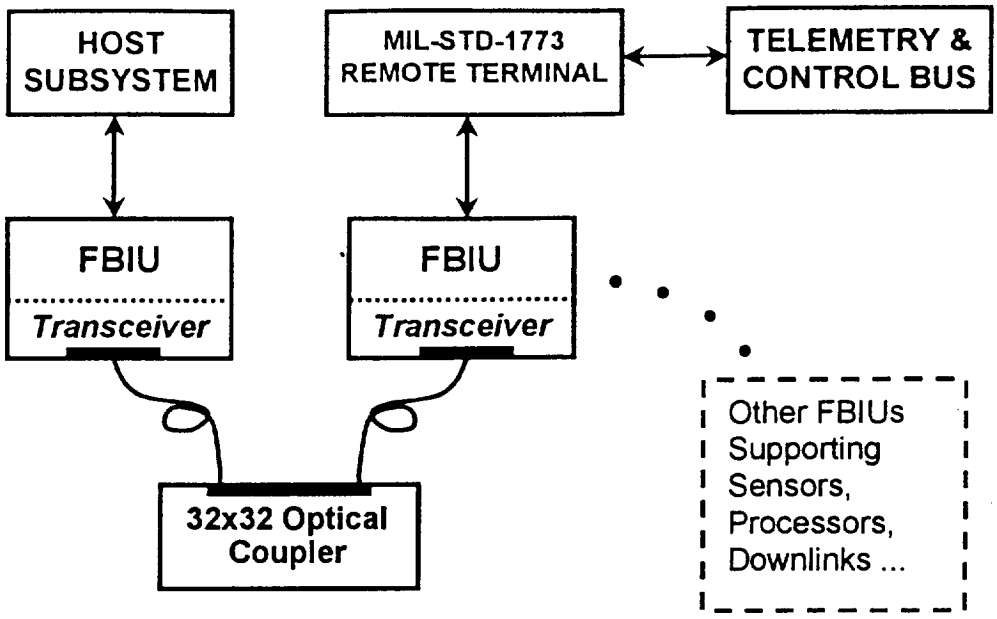


Figure 5.6. Schematic of a STAR FODB network.

- Total ionizing dose (TID): long term degradation of device performance, which eventually leads to device failure.
- Examples of single event effects (SEEs):
  - SEL, SEGR, SEB: single cosmic ray particle event that can cause the device to stop functioning. In some cases like SEL this is recoverable.
  - SEU, SET: Single particle induced change in the logic-state of a digital device (SEU) or a temporary change in the output state of a analog device (SET). Bit errors in a data stream can be a manifestation of an SET in an photodiode.
- Displacement damage: long term degradation of device performance, which eventually leads to device failure.

This section deals with the topic of *in situ* testing of full functional optical data links. First, as an example, proton testing on a specific optical system will described. Then, results from several different optical system tests will be listed.

### 5.1.3.1 Proton-Induced Bit Error Response of a Fiber-Optic System

This section will describe radiation effects bit error study carried out on the Boeing-designed STAR Fiber Optics Data Bus (FODB) [Dale-96]. The STAR FODB [Dale-96] is a 200 Mbps 32 node star coupled fiber based data bus. The star coupler is dual

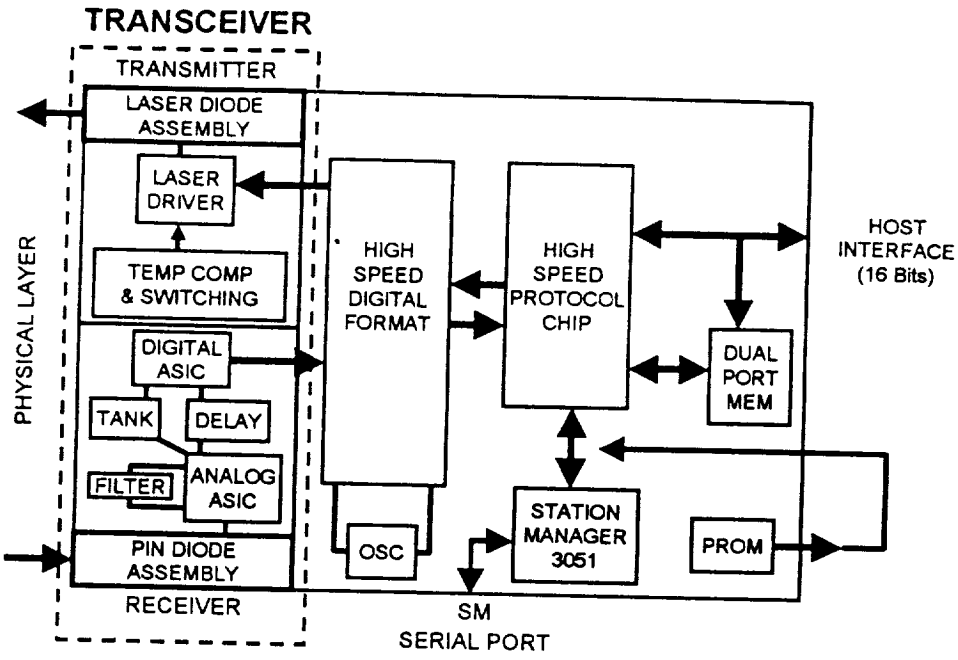


Figure 5.7. Schematic of a fiber optic bus interface (FBIU).

redundant, the data stream is Manchester encoded, the system also allows for error checking. It utilizes 1300 nm optoelectronics.

**Figure 5.6** is a block diagram of a generic application of the STAR FODB [Dale-96]. The fiber bus interface unit (FBIU) contains a transceiver (the transmitter and receiver) and support circuitry necessary to implement the protocol and form the host interface. Each subsystem FBIU is connected to all others via the 32x32 optical star coupler. A block diagram of the FBIU is given in **Figure 5.7**.

A detail description of the FBIU can be found in [Frit-94]. Some of the key components are listed next. The photodiode is a 1300 nm laser diode and the photodetector is the Epitaxx EXT75 PIN. The data formatter is a high speed GaAs ASIC that formats and deformats, encodes and decodes, and performs error checking. The protocol chip is a CMOS ASIC. The station manager is a CMOS micro-controller. The dual port memory is 3.3 V CMOS RAM. It should be obvious to the reader that there are several different issue that should be address when qualifying this hardware for use in the space radiation environment. Each device should be reviewed for its performance

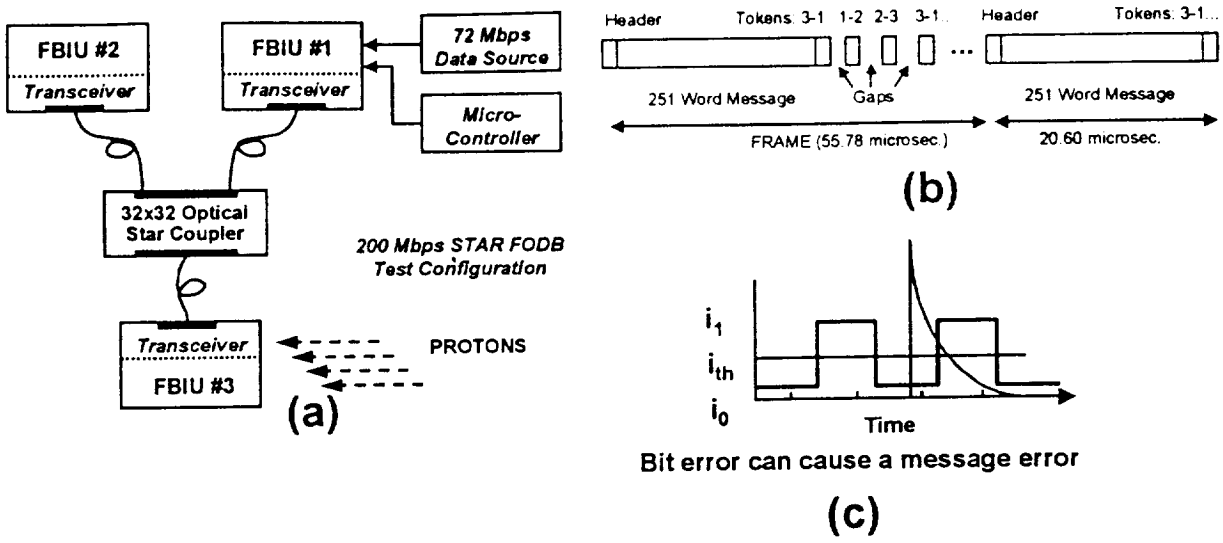


Figure 5.8. (a) Configuration of three FBIUs during proton system testing. (b) message packet used during test. (c) SET induced bit error leads to message error.

degradation. Here we will describe some of the result from a proton-induced bit error characterization study.

An example of a system level proton test on the STAR FODB is shown in **Figure 5.8.A** [Dale-96]. The test network configuration included three FBIUs, one of these was selected for irradiation. In order to completely test the system protocol all three FBIUs must be used. System errors are defined by the bus protocol [Frit-94]. Error logging during an irradiation is automatic. **Figure 5.8.B** depicts the messages transfers used for these tests. Each frame has a 251 word long message, each word is 16 bits. When messages were not being sent, a sequence of tokens was passed around the network. For these tests a message error was defined as any loss of data, that is any event that changes a bit in the message packet **Figure 5.8.C**. Errors in tokens were not counted as message errors.

A sequence of exposures was carried out that stepped through each component [Dale-96]. The measured error cross-sections for the entire transceiver are given in **Figure 5.9** as the triangles. Comparing this to results obtained on the photodiode module (upside down triangles) shows that a large portion of the events are due to events in the photodiode. The squares in this figure give the error cross-section measured on the

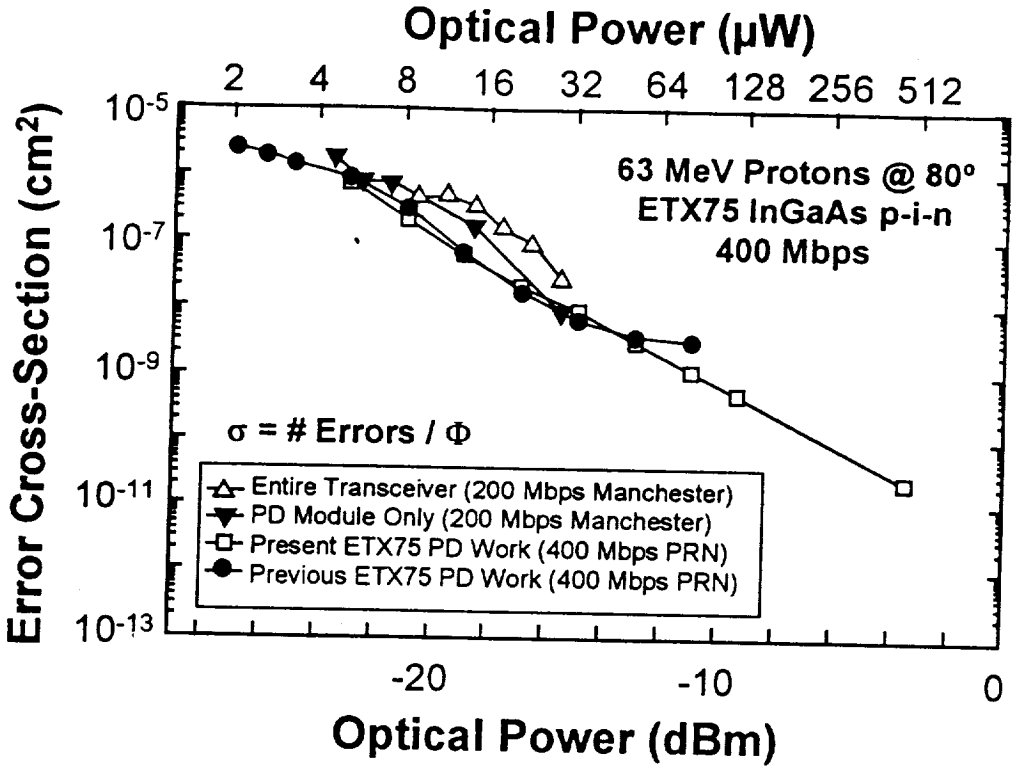


Figure 5.9. Comparison of message error cross-section to error cross-section of photodiode.

photodiode from the generic BER tests, **Figure 5.3**. In this case the system errors are well defined by the generic BER test results on the photodiode.

Results from proton exposures of other components are detailed in [Dale-96] we summarize them here. A small number of errors occurred when the protocol chip and the data formatter were exposed to more than 20krad(Si) of protons. No errors occurred during exposures of the station manager. The dual port memory was not tested during the system test, however proton and heavy ion SEE testing and TID testing was carried out independently in [Dale-96]. The impact of TID on message error rate was also characterized. For this system configuration, device TID-induced degradation was a limiting factor for certain spaceflight missions.

Several other system or quasi-system level tests have been performed [LaBe-98, Cart-97, Mars-96, Mars-94a, LaBe-94, Mesh-93, LaBe-93]. The reader is encouraged to

review these publications, they give detail discussion of the test setup and results. We summarize some of the effects observed here:

- Transients in photodiode dominate BER
- TID effects at dose near 20 krad(Si)
- SEU in support circuitry can dominate BER
- Certain system errors can be flux dependent, i.e. system that utilize message retries
- Unexplained high current condition in transmitter
- SEU in logic portion cause the link to stop functioning, required a re-initialization

The results of these fiber-optic data link radiation tests show the need to carefully characterize each component of the fiber-optic data link for selected SEE, TID and displacement damage effects, see Section 3.0. Some of these effects should be characterized at the system level, while others can be characterized at the component level. Any device that can impact the system performance by causing system message errors should be well characterized under system-like environment. The on-orbit message error rate will depend on the message packet size, system message encoding, error checking and correction, and other system characteristics.

We should stress here that each *in situ* test poses specific challenges, the test team should carefully weigh each segment of the test plan carefully based on the requirements and functionality of the system under test. Some of these considerations are listed below:

- Determine limitations when performing system level heavy ion and proton testing, e.g., packaging may limit heavy ion bit error testing and TID may limit proton testing
- Understanding of system mitigation approaches and how these will impact testing
- Component level TID testing to quantify the risk for failure, e.g. parametric and functional failure of support ASICs, RAM or other support device
- Component level SEE testing, e.g. SEL screening or heavy ion bit error testing
- Knowledge of range of optical power launched on photodiodes in the network
- Orientation of the photodiode in receiver package
- During proton bit error testing the optical power launched on the photodiode can be degraded due to darkening of passive components exposed to the beam or loss of responsivity of the photodiode itself

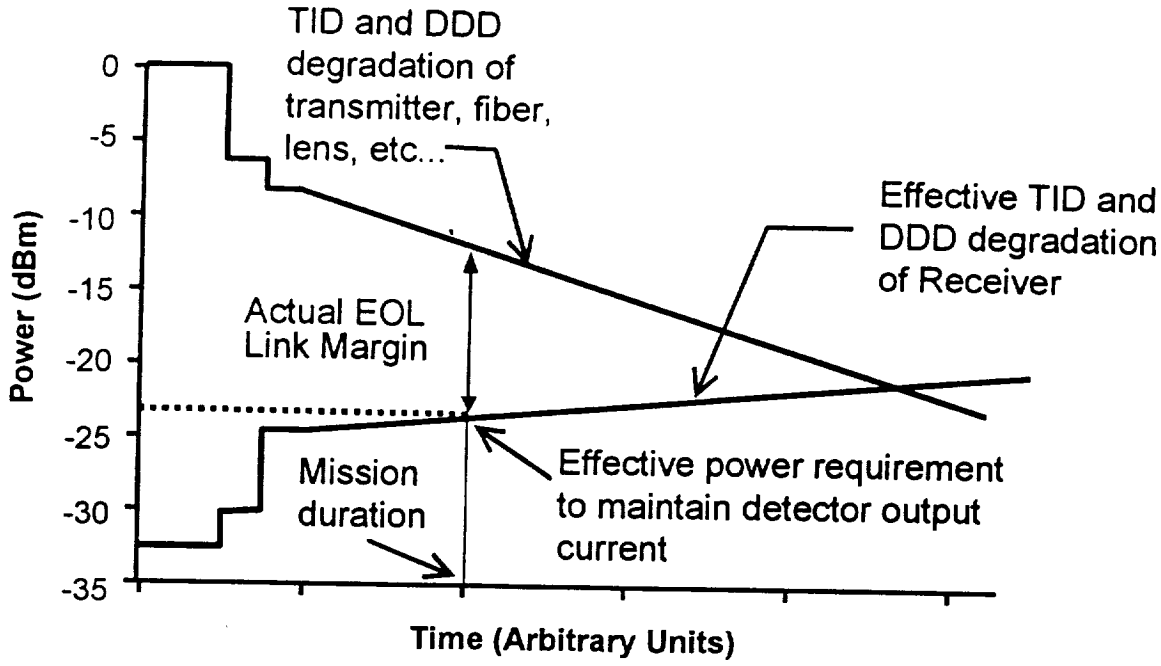


Figure 5.11. Radiation induced degradation of power budget margin

## 5.2 Assessing Radiation Effects at the System Level

Assessing performance of an optical data link in the space radiation environment requires one to consider the affects of TID, displacement damage and SEE on system performance metrics described in Section 3.3. In general, system level assessment of radiation effects on spaceflight hardware has been the described in [Kinn-98, LaBe-96]. In this section we discuss the issues that are specific to fiber optic data links. First we consider the how TID and displacement damage impacts the power budget. Next we discuss the techniques for predicting on-orbit BER, and impact of power budget on BER. A brief discussion of bit-error mitigation approached is given next. And finally, we will present on-orbit performance of some fiber optic data buses.

### 5.2.1 TID and Displacement Damage Impacts on Power Budget

A power budget analysis for an optical fiber link was demonstrated in Section 3.3. This kind of analysis gives the pre-launch power budget margin for the system, see **Figure 5.10**. The abscissa is labeled in arbitrary units of time (instead of length as in

**Figure 3.14**). As a fiber-based system is exposed to the space radiation environment the power budget margin will decrease. This is due to several effects. **Figure 5.11** shows graphically how these effects impact link margin. The slope of the top line represents idealized TID and displacement damage effects as the mission time increases. Some of the effects are degradation of source optical power and the signal as it passes through the fiber and optics components like lenses. The slope of bottom line represent idealized TID and displacement damage impacts on the optical power needed to maintain the required system BER, for example displacement damage degradation of the responsivity of the photodiode.

An example mission life is marked on the time axis. The power launched on the detector at the end of the mission life will be –12 dBm. The power requirement for maintaining system BER is –23dBm. The net end of life (EOL) link margin is 11 dB. This type of power budget margin analysis for fiber-optic data links that will be used in the space radiation environment is required to ensure that the EOL margin is sufficient to maintain a functioning optical link.

### 5.2.2 Impacts of Radiation-Induced Bit Errors on On-Orbit BER

Traditional proton-induced on-orbit error rate calculations [Pete-97] assume indirect ionization is the dominant mechanism for upset. The error cross-section is measured at various proton energies. These data are then fit using Bendel curves. The error rate is computed by direct integration of the on-orbit flux-energy curves with the Bendel curve fit to the error cross-section data.

Traditional heavy ion-induced error rate calculations [Pete-97] assume that direct ionization is the dominant mechanism for upset. The error cross-section is measured at various effective LETs, then fit using Weibull distribution. The error rate is computed using right rectangular parallelepiped model for sensitive volume, Weibull distribution and LET spectra.

All traditional approaches for computing on-orbit error rates separate direct and indirect ionization effects. The traditional methods of predicting error rates are appropriate for almost any device used in fiber optic data links, one exception to this is proton-induced error rate prediction for bit errors in photodiodes.

### 5.2.2.1 Proton-Induced Bit Errors in Photodiodes and On-Orbit BER

Direct ionization can dominate proton-induced optical data link bit errors that result from SETs in the photodiode, see in Section 5.1.2.1 and Section 4.3.2. Traditional approaches that assume indirect ionization effects only when predicting proton-induced BER will not work for proton events in photodetectors. Accurate predictions of SETs in a photodiode must include a combination of direct and indirect effects [Marsh94a, Johnston98].

In [Marsh94a] suggests using a combination of the existing tradition methods, i.e., use ground data to delineate the angle where direct ionization effects begin to dominate the cross-section, then apply traditional approach for direct ionization effects for grazing angles greater than this cutoff and indirect effects for angle less then this cutoff. In [Johns98] an empirical approach was suggested that requires data to be collected at several angles of incidence and at several proton energies, then integration of these data over the proton spectra. A detail formulation for computing error rates in photodiodes that incorporates direct and indirect ionization effects has not been published.

Typically, proton-induced error cross-section data are collected as a function of proton energy (not proton LET) for devices like Random Access Memories (RAMs). For these device types the mechanisms for upsets are classically dominated by nuclear reactions. However, this is not the case for photodiodes, where the mechanism for upset are some combination of nuclear reactions (or indirect ionization) and direct ionization, and can be dominated by direct ionization. Below we describe a common approach used for optical fiber links that show bit errors that are dominated by direct ionization from protons.

Reference [Mars-94a and Mars-99] shows that for fiber link applications that are very sensitive to the proton-induced effects bit error data can be analyzed in terms of particle LET. The standard methods for correcting for the increased path length of an ion through the sensitive volume and the decrease of the area of the sensitive volume projected perpendicular to the beam were applied to the proton and He data. The result is a very convincing plot showing that it is possible delineate the data using the conventional methods of computing effective LET and error cross-section by fitting a Weibull

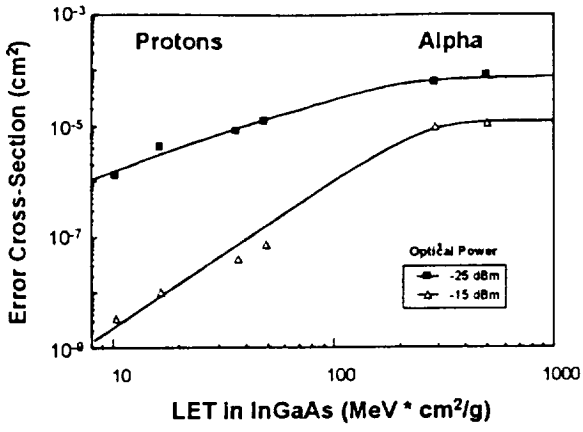


Figure 5.12. Plot of the 400 Mbps data in Figures 5.4 and 5.5 using conventional techniques to correct LET and cross-section for beam angle

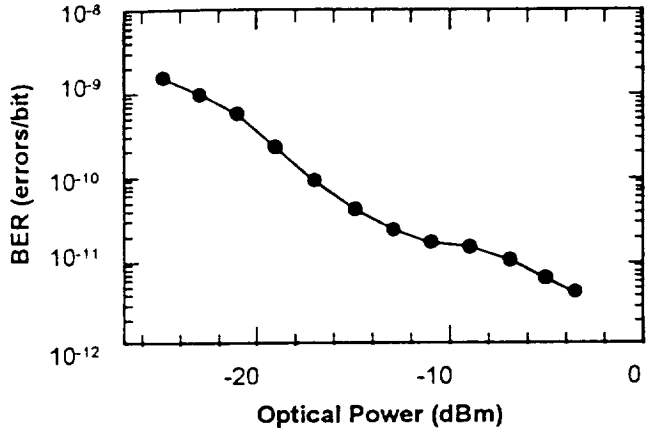


Figure 5.13. On-orbit BER during solar particle event at various optical powers

distribution to the data, see **Figure 5.12**. This plots the cross section for a bit error while operating at the link 400 Mbps over various values of effective LET in InGaAs (note units are MeV $cm^2$ / g). The data for LETs > 100 are from proton exposures, data > 100 are He exposures.

Predicting the proton-induced on-orbit bit error rates using data like that in **Figure 5.12** was demonstrated in [Mars-94a, Mars-96]. The approach was to determine the best Weibull fit to the data and use the standard tools for determine the heavy ion induced (i.e. direct ionization) error rate [Pete-97]. **Figure 5.13** shows the results of this type of calculation over various optical powers for a 400 Mbps application during a solar particle event. Recall that these error cross-section data varies with data rate, any rate calculation (on any clocked device) must consider the application operating frequency [Mars-94a, Reed-96]. This type of calculation assumes that bit errors are dominated by direct ionization effects at all angles.

### 5.2.2.2 System BER Considerations

The BER of an optical system operating outside of a radiation environment is determined by several factors, one important factor is the optical power launch on the photodiode. The previous sections and references contain in them demonstrate that the

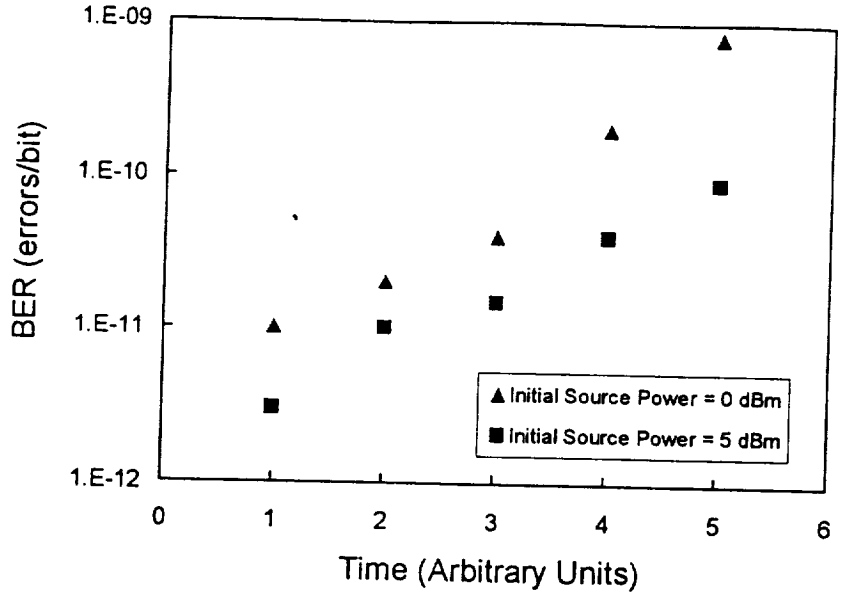


Figure 5.14. SEE-induced bit errors can be accommodated by increasing link margin by increasing source power.

radiation induced BER is also a function of optical power. Consider the case where the optical power launched on the photodiode is degrading over time as shown in the top curve in **Figure 5.11**. Also assume that the receiver does not degrade, that is the photodiode and follow-on circuitry response is identical to that the day the spacecraft was launched. Further assume that **Figure 5.13** determines the on-orbit average BER during a solar particle event. Finding the optical power at various points along the mission duration **(Figure 5.11)** and using that optical power to determine the proton-induced BER **(Figure 5.13)** gives the increase in proton-induced BER over the mission life, this is plotted as the triangles **Figure 5.14**. The squares are the same had the initial source optical power been 5 dBm. In this example, operating the source output 5 dB higher decreases the radiation induced BER by up to an order of magnitude.

### 5.2.3 Bit Error Mitigation Approaches

There are many ways to mitigate bit errors, this can be done at the component level or system level [LaBe-98]. There are most always performance trades that must be made when implementing mitigation approaches. Some examples are described here:

- Reduce detector depletion layer thickness. This decreases the target size and limits charge collection. Indirect band gap (Si) diodes have thicker depletion regions than direct band gap (III-V) diodes.
- Another component level solution is to reduce the photodiode area, again reducing the target size. Limitations on received optical power limit the amount of area reduction that is possible.
- Over-sampling and comparing a single data bit. Over-sampling is not possible at high data rates (~ >100 Mbps) where the duration of the transient event is on the same order as a bit period.
- Encoding, parity checking for error detection. Enabling of retry commands for error correction. The impact is an effective 50% loss of bandwidth.Requires buffer memory and handshaking architecture. Difficult to implement in high data rate systems

### 5.2.4 On-Orbit Use of Fiber-Optic Data Links

Several optical components and optical links have been used or tested in spaceflight hardware over the past several years, the Long Duration Exposure Facility (LDEF) in 1978 [John-92] was the first experiment of fiber-optics in space. In 1993 Boeing carried out the first analysis of on-orbit bit errors in a operation fiber optic link [Cros-93].

The NASA Small Explorer Program's implementation of a fiber-optic data bus, named Small Explorer Data System (SEDS), was used to transfer telemetry and commands between subsystems. The standards community identifies the SEDS fiber-optic system structure as MIL-STD-1773. This 1 MHz bus is slave/master configuration that has two sides, side A and the redundant side B. The messages are Manchester encoded and can be up to 32 words long. In 1995 the standard was revised to include data transmission at 1 Mbps or 20 Mbps, it was renamed to AS-1773 [A-1773]. The functional requirements of AS-1773 remained the same as MIL-STD-1773. A detailed discussion of the bus protocol can be found in [A-1773]. One notable error detection and correction feature is that after every received message the receiving node sends a short return message to the master identifying the status of the received message. The status message tells the master to retransmit the message if the first transfer was unsuccessful.

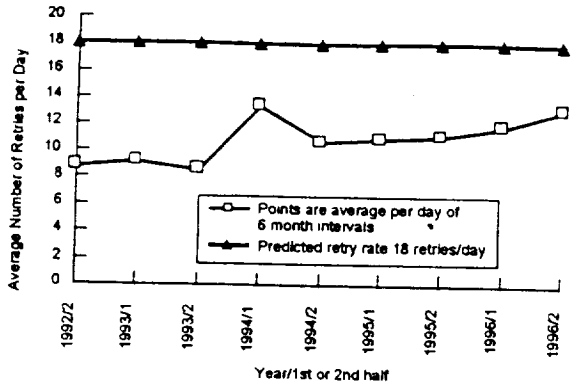


Figure 5.15. Comparison for predicted retry rate to the measured value for SEDSI on SAMPEX

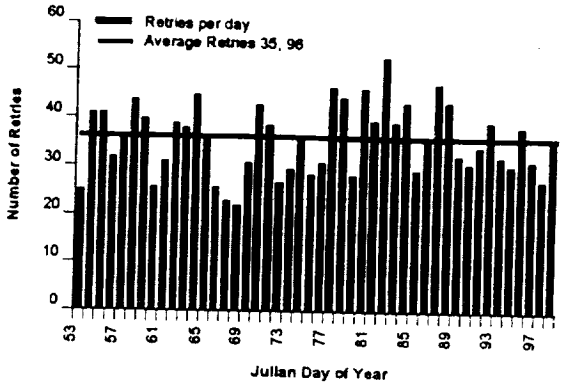


Figure 5.16 Comparison for predicted retry rate to the measured value for SEDSI on SAMPEX

The first generation SEDS (SEDSI) data bus was used on NASA's Solar Anomalous Magnetospheric Particle Explorer (SAMPEX). SAMPEX was launched in July 1992. The SEDSI radiation test effort is described in [LaBe-93]. The second generation of SEDS (SEDII) was used on the Hubble Space Telescope (HST) Solid State Recorder (SSR). The SSR was installed on HST Feb 1997. A comparison of the radiation performance of the first and second generation SEDS data bus was given in [LaBe-97]. This work compared on-obit bit error data to prediction made from proton-induced ground data. The ground data was identical for the two generations, this is not unexpected because the major changes to the link were mechanical and electrical, the same optical components were used in both generations. The next two paragraphs summarize the observed on-orbit performance.

The operation of SEDSI on SAMPEX has been successful. No bus outages or failed messages have occurred. However, there has been several data bit that have been corrupted requiring the message be retransmitted. The number of message retransmissions is shown in **Figure 5.15** [LaBe-97]. This figure also shows the predicted number of retransmissions. Most of the retransmissions have occurred in the SAA.

The number of bus SSR SEDSII retransmissions per day for the first two months of operation is plotted in **Figure 5.16** [LaBe-97]. SEDSII on HST is fully operational. No bus outages have occurred. There have been several retransmission failures, the frequency is about 1 every 2 days. This is believed to be due to software or hardware

error. An error cross-section calculation and on-orbit prediction approach for multiple retransmissions based on a Binomial distribution for the retry probability and the cross section for single message errors was developed in [LaBe-93, and revisited in LaBe-97].

## 6.0 Radiation Effects in Emerging Optical and Optoelectronic Technology

This section will focus on recent radiation effects testing of technology that could eventually be used in digital optical data transfer system in spaceflight applications. This section is intended to give the reader a sense of radiation effects issues for state-of-the-art of the technology. As with any text that attempts to describe the emerging technology, this text will most likely be out of data by the time of its printing.

[LaBe-98] listed vertical cavity service emitting laser (VCSEL) and metal-semicondictor-metal (MSM) photodetector as two technologies that have strong potential for use in spaceflight high-speed optical data link. VCSEL are high-speed small-scale (< 10 μm diameter) top emitting lasers. These devices can be fabricated to form an array of light emitters with each having very small beam divergence. Proton-induced radiation effects testing of VCSELs can be found in [Barn-99]. These data show excellent performance for most spaceflight applications. MSMs are high-speed (10s-100s GHz) photodetectors. Like VCSELs they are small-scale and can be fabricated to form arrays. Proton-induced tests on MSM [Mars-99] show the same trends for SETs in photodiodes, see Section 4.3.2, were very robust to TID and DDD effects.

Several commercial vendors have developed fiber optic transceivers. A world wide web search on May 25, 2000 for "fiber optic transceiver" uncovered over 1200 pages. The list below is a subset of the list of vendors.

- Telebyte, Inc http://www.telebyteusa.com/index.htm
- TC Communications http://www.tccomm.com/LAN.htm
- 3Com http://www.3com.com
- Agilent Technologies (HP) http://www.agilent.com/
- Lasermate Corporation http://www.lasermate.com/

These transceivers could easily use technologies that are very robust to the space radiation environment. Careful radiation effects characterization should be carried out to evaluate the transceiver susceptibility to TID, DDD, and SEE.

High speed (> 1 GHz) support electronics are required for Gbps data rates and beyond. GaAs MESFET and Bipolar emitter-coupled logic (ECL) are mature technologies that can operate in the GHz regime. Other III-V and Si semiconductor

technologies are currently under development. TID testing on GaAs, ECL, SiGe, InP, and CMOS SOI has proven these technologies to be sufficiently robust to space environment TID effects. Testing on ECL and GaAs technologies has shown them to be SEU sensitive. Growing GaAs with a buried layer at low temperatures has shown to be effective at mitigating SEUs. SEU sensitivity of other technologies is yet to be determined.

A glance at these technologies and the associated radiation effects issues shows that the future for high-speed (>1Gsps) optical data links in spaceflight application is very promising. It will not be without its challenges, from a design perspective as well as a radiation effects issues. SEU and SET effects are certain to be one of the more complex issues that engineers and radiation effects researchers will face in implementing these technologies into spaceflight hardware.

## 7.0 Summary and Conclusions

We began this segment of the Short Course by giving a brief overview of the space radiation environment, summarizing the basic space radiation effects important for microelectronics and photonics and giving an example of a typical mission radiation environment requirements.

We then gave an overview of intra-satellite digital optical data link systems that included a discussion of the digital optical data link, some link components, and a brief description of optical link power budget and bit error ratio.

Then we gave a discussion of radiation effects in optical and optoelectronic components that the focused on degradation of passive optical components and SEE in photodiodes. We presented information on DDD degradation on source output power and laser turn-on threshold. We discussed in some detail the characterization of TID attenuation of signal via darkening in passive transmission medium. We also reviewed the fact that radiation-induced transients in photodetectors is the major consideration for high speed data links, while DDD degradation of detector output current and TID and DDD increase in background noise are second order effects. We note here once again that radiation effects in support circuitry is outside of the scope of this segment of the short course. However, TID and DDD parametric and functional failure, SEU in logic, SEL in CMOS, and SET in linear devices can be a major issue in when considering the system performance of a data link when exposed to the radiation environment.

We then presented a section that focused on optical data link system response to the space radiation environment. First a discussion of system level SEE ground testing was given that stressed the importance of understanding how radiation induced bit errors in any device in the data path can add to the system BER. SETs in photodiodes pose specific challenges due to mixed effects of direct and indirect ionization. Cross-section measurements must be made of over angle, optical power and operating frequency. We also demonstrated that other support circuitry can show frequency dependence. *In situ* BER/MER testing at system level is required to determine how device level effects impact system performance, e.g. the system may or may not respond device effect. A variety of system effects have been observed where the limiting factors can be TID,

DDD, SEE or some combination. SETs in photodiode have been shown to be a major issue for several digital optical data links.

The system level ground-based characterization discussion was followed by a discussion of system level assessment of the data link performance when operating in the space radiation. We show the importance of managing TID and DDD effects in sources and passive transmission media. These effects can be avoided via device selection and/or mitigated via optical power budget management. Predicting on-orbit BER from radiation effects in support electronics can be done using standard on-orbit error rate calculation tools. However, for photodiodes, one must use a modified approach for on-orbit BER prediction that includes direct ionization effects from protons. Radiation-induced increases in system BER mitigation can be done at device, circuit, or system level.

The bottom line is : Designers must consider radiation effects concerns when making decisions about network configuration (Cu vs optical, star vs linear, 1300nm vs 850nm, ...). These trades studies must include impacts that device selection and configuration has on radiation response. Once a system configuration is selected the system response must be assessed for TID, DDD and SEE impacts.

## 8.0 Acknowledgments

We would like to thank each person in the Radiation Effects and Analysis Group and the Radiation Physics Office at NASA Goddard Space Flight Center for their support. Specifically we would like to thank Paul Marshall, Ken LaBel, Cheryl Marshall, and Janet Barth for their insightful technical discussions and guidance, this course would not of been possible had they not been willing to let us tap into their vast knowledge of this subject matter. Thank you. We would also like to thank Martha O'Bryan for her support in formating of the graphics and text in the written and oral presentation of this short course.

Like most of our adventures, we would not of completed this one had it not be for the forgiving support of our families.

## 8.0 References


[A1773] The Society of Automotive Engineers (SAE), as an industry-related standards entity,has adopted the MIL-STD-1773A standard (with modifications) and now support this new SAE standard as "Fiber optic mechanization of a time division multiplex data bus," AS-1773, SAE, 1995.

[Agra-97] G. P. Agrawal, Fiber-Optic Communication Systems, 2nd edition, New York, Wiley, c1997.

[Barn-82] C.E. Barnes, "Neutron damage effects in laser diodes,"Proc. SPIE, vol. 328, pp. 88-94, 1982.

[Barn-84] C.E. Barnes and J. J. Wiczer, "Radiation effects in optoelectronic devices," Sandia Report, SAND84-0771, 1984.

[Barn-86] C. E. Barnes, "Radiation hardened optoelectronic components: sources," *Proc. SPIE,* vol. 616, pp. 248-252, 1986.

[Barn-90] C. Barnes, L. Dorsky, A. Johnston, L. Bergman, and E. Stassinopoulos, "Overview of fiber optics in the natural space environment," in *Fiber Optics Reliability: Benign and Adverse Environments IV, Proc. SPIE,* 1990, vol. 1366, pp. 9-16.

[Bart-97] J. Barth, "Modeling space radiation environments," Notes from 1997 IEEE Nuclear and Space Radiation Effects Conference Short Course.

[Bend-84] W.L. Bendel and E.L. Petersen, "Predicting single event upsets in the earth's proton belts," IEEE Trans. on Nucl. Sci., vol. NS-31, no.6, pp. 1201-1207, 1984.

[Bris-93] J. Bristow and J. Lehman, "Component tradeoffs and technology breakpoints for a 50 Mbps to 3.2 Gbps fiber optic data bus for space applications," *Proc. SPIE,* vol. 1953, pp. 159-169, 1993.

[Burk-87] E. A. Burke, C. J. Dale, A. B. Campbell, G. P. Summers, T. Palmer, and R. Zuleeg, "Energy dependence of proton-induced displacement damage in GaAs," IEEE Trans. on Nucl. Sci., vol. NS-34, no.6, pp. 1220-9, 1987.

[Chap-93] M. de La Chapelle, A. W. Van Ausdale, and M. E. Fritz, "The STAR-FODB (fiber optic data bus) program," in *Proc. GOMAC '93 Conf.,* pp. 395-397.

[Cros-93] D. Cross, M. Fritz, D. Haakenson, C. Hoeflein, R. Hodges, S. Kelnhofer, J. Lam, and M. Summerhays, "The Boeing photonics space experiment," *Photonics for Space Environments I,* vol. SPIE-1953, pp. 116-26, 1993.

[Dale-89] C. J. Dale, P. W. Marshall, G. P. Summers, and E. A. Wolicki, "Displacement damage equivalent to dose in silicon devices," Appl. Phys. Lett., vol. 54, no.5, pp. 451-3, 1989.

[Dale-92] C. J. Dale , and P. W. Marshall, "Radiation response of 1300 nm optoelectronic components in a natural space environment," Proc. SPIE, vol. 1791, pp. 224-232, 1992.

[Dale-95] C. J. Dale, P. W. Marshall, K. A. Clark, M. de La Chapelle, M. E. Fritz, and K. A. LaBel, "Fiber optic data bus space experiment on board the microelectronics and photonics test bed (MPTB)," *Photonics for Space Environments III,* vol. SPIE-2482, p. 285, 1995.

[Dale-96] C. J. Dale, P. W. Marshall, M. E. Fritz, M. de La Chapelle, M. A. Carts, and K. A. LaBel, "System radiation response of a high performance FODB," IEEE Trans. on Nucl. Sci., vol. NS-43, no.3, p 1030, 1996.

[DeCu-98] C. DeCusatis, Handbook of Fiber Optic Data Communication, San Diego, Academic Press, c1998.

[DeRu-93] J.DeRuiter, "Survivable ring architecture for spaceborne applications," *Proc.SPIE,* vol. 1953, pp. 128-135, 1993.

[Dodd-99] P. Dodd, "Basic mechanisms for single event effects," Notes from 1999 IEEE Nuclear and Space Radiation Effects Conference Short Course.

[Dres-98] P. V. Dressendorfer, "Basic mechanisms for the new millenium," Notes from 1998 IEEE Nuclear and Space Radiation Effects Conference Short Course.

[Dyer-98] C. S. Dyer, "Space radiation environment dosimetry," Notes from 1997 IEEE Nuclear and Space Radiation Effects Conference Short Course.

[Frie-85] E. J. Friebele, K. J. Long, C. G. Askins, M. E. Gingerich, M. J. Marrone, and D. L. Griscom, "Overview of radiation effects in fiber optics,"*Crit. Rev. Tech.:Opt. Materials in Radiation Environ.*, P. Levy and E. J. Friebele,Ed. Bellingham, WA: SPIE, 1985, vol. SPIE-541, pp. 70-88.

[Frie-91] E.J. Friebele, "Photonics in the space environments," Notes from 1991 IEEE Nuclear Space Radiation Effects Conference Short Course.

[Frit-94] M.E. Fritz, B.E. Daniels, M. de La Chapelle, D.A. Cross, A.W. Van Ausdale, "The STAR FODB program," SPIE Proc. on Photonics for Space Environments II, vol. 2153, 1994.

[Frit-95] M.E. Fritz, M. de La Chapelle, and A. W. Van Ausdale, "Boeing's STAR FODB test results," *Photonics for Space Environments,* vol. SPIE-2482, pp. 226-235, 1995.

[Gris-94] D. L. Griscom, M. E. Gingerich, and E. J. Friebele, "Model for dose, dose-rate, and temperature dependence of radiation induced loss in optical fibers," *IEEE Trans. Nucl. Sci.,* vol. NS-41, no. 3, pp. 523-527, 1994.

[Gros-93] S. Gross, "ATM-based protocol for Gbps ring networks," in *Proc. Gomac '93 Conf.*, p. 399.

[Hous-98] S.L. Houston and K.A. Pfitzer, "A new model for the low altitude trapped proton environment," IEEE Trans. on Nucl. Sci., vol. NS-45, no.6, pp. 2972-2978, 1998.

[Jord-93] A.F. Jordan, "On the brink: Fiber optic LAN's for avionics and space," *Defense Electronics,* vol. 25, no. 11, pp.43-47, 1993

[John-92] A.R. Johnston and E.W. Taylor, "A survey of the LDEF fiber optic experiments," JPL Report D-10069, Nov. 10, 1992.

[Kinn-98] J.D. Kinnison, "Achieving reliable, affordable systems" Notes from 1998 IEEE Nuclear and Space Radiation Effects Conference Short Course.

[LaBe-91] K. LaBel, E. G. Stassinopoulos, and G. J. Brucker, "Transient SEU's in a Fiber Optic System for Space Application," IEEE Trans. Nucl. Sci., vol. 38,no. 6,1991.

[LaBe-93] K.A. LaBel, P. Marshall, C.Dale, C.M. Crabtree, E.G. Stassinopolous, J.T. Miller and M.M. Gates, "SEDS MIL-STD-1773 fiber optic data bus: Proton irradiation test results and spaceflight SEU data," *IEEE Trans. Nucl. Sci.*, vol. 40, no. 6, pp. 1638-44, 1993.

[LaBe-94] K. A. LaBel, D. K. Hawkins, J. A. Cooley, C. M. Seidleck, P. Marshall, C. Dale, M. M. Gates, H. S. Kim, and E. G. Stassinopoulos, "Single event effect ground test results for a fiber optic data interconnect and associated electronics," *IEEE Trans. Nucl. Sci.*, vol. 41, no. 6, pp. 1999-2004, 1994.

[LaBe-96] K.A. LaBel, and M.M. Gates, "Single-Event-Effect mitigation from a system perspective," *IEEE Trans. Nucl. Sci.*, NS-42, no. 2, pp. 654-660, April 1996.

[LaBe-97] K.A. LaBel, R.A. Reed, H. Leidecker, J. Barth, P.W. Marshall, C.J. Marshall, C. Seidleck, "Comparison of MIL-STD-1773 fiber optic data bus terminals: single event proton test irradiation, in-flight space performance, and prediction techniques," IEEE Trans. on Nucl. Sci., NS-44, no. 3, 1998.

[LaBe-98] K.A. LaBel, Notes from 1998 IEEE Nuclear and Space Radiation Effects Conference Short Course.

[Lach-98] G. Lachs, Fiber Optic Communications : Systems, Analysis, and Enhancements, New York, McGraw-Hill, c1998.

[Lisc-92] H. Lischka, H. Henschel, W. Lennartz, and H. U. Schmidt, "Radiation sensitivity of light emitting diodes, laser diodes, and photodiodes," IEEE Trans. Nucl. Sci., vol. NS-39, no. 3, pp. 423-27, 1992.

[Mars-89] P. W. Marshall, C. J. Dale, G. P. Summers, E. A. Wolicki, and E. A. Burke, "Proton, neutron, and electron induced displacement damage in Germanium," IEEE Trans. on Nucl. Sci., vol. NS-36, no. 6, pp. 1882-9, 1989.

[Mars-92] P. W. Marshall, C. J. Dale, and E. A. Burke, "Space radiation effects on optoelectronic materials and components for a 1300 nm fiber optic data bus," *IEEE Trans. Nucl. Sci.*, vol. 39, no. 6, pp. 1982-1989, 1992.

[Mars-93a] P. Marshall, J. Cutchin, and T. Weatherford, "Space radiation effects in a GaAs C-HIGFET logic family suitable for satellite data transmission above 1 Gbps," in *Proc. GOMAC '93 Conf.*, pp. 227-229.

[Mars-93b] P. Marshall, C. Dale, and K. LaBel, "Charged particle effects on optoelectronic devices and bit error rate measurements on 400 Mbps fiber based data links," in *Proc. RADECS Conf.*, Saint Malo, France, Sept. 13-16, 1993, pp. 266-271.

[Mars-93c] P.W. Marshall, K.A. LaBel, C.J. Dale, J.P. Bristow, E.L. Petersen, and E.G Stassinopoulos, "Physical interactions between charged particles and optoelectronic devices and the effects on fiber based data links," Proc. SPIE, vol. 1953, pp. 104-115, 1993.

[Mars-94a] P. W. Marshall, C. J. Dale, M. A. Carts, and K. A. LaBel, "Particle induced bit errors in high performance data links for satellite data management," *IEEE Trans. Nucl. Sci.*,vol. NS-41, no.6, pp. 1958-65, 1994.

[Mars-94b] P. W. Marshall, C. J. Dale, E. J. Friebele, and K. A. LaBel, "Survivable fiber-based data links for satellite radiation environments," *SPIE Critical Review CR-14, Fiber Optics Reliability and Testing*, pp. 189-231, 1994.

[Mars-96] P.W. Marshall, C.J. Dale, and K.A. LaBel, "Space radiation effects in high performance fiber optic data links for satellite management," *IEEE Trans. Nucl. Sci.*,vol. NS-43, no.3, pp. 645-653, April 1996.

[Mesh-94] D. C. Meshel, G. K. Lum, P. W. Marshall, and C. J. Dale, "Proton testing of InGaAsP fiber optic transmitter and receiver modules," in *Proc. IEEE Radiation Effects Workshop*, 1994, NSREC 64-76.

[Mars-99] P.W. Marshall and C.J. Marsahll, "Proton effect and test issues for satellite designers," Notes from 1999 IEEE Nuclear and Space Radiation Effects Conference Short Course.

[Pala-98] J. C. Palais, Fiber Optic Communications, 4th edition, Prentice Hall, Upper Saddle River, N.J., c1998.

[Pete-97] E.L. Petersen, "Single event analysis and prediction," Notes from 1997 IEEE Nuclear and Space Radiation Effects Conference Short Course.

[Ritte-93] J. C. Ritter, "The microelectronics and photonics test bed (MPTB)," *Photonics for Space Environments I*, vol. SPIE-1953, pp. 2-6, 1993.

[Rose-82] B. H. Rose, and C. E. Barnes, "Proton damage effects on light emitting diodes," J. Appl. Phys., vol. 53, no. 3, pp. 1772-80, 1982.

[Smith-90] B.S. Smith, "SEDS segment specification for a MIL-STD-1773 data bus system for the small explorer data system," NASA GSFC-730-89-011, 1990.

[Summ-87] G. P. Summers, E. A. Burke, C. J. Dale, E. A. Wolicki, P. W. Marshall, and M. A. Gehlhausen, "Correlation of particle-induced displacement damage in silicon," IEEE Trans. on Nucl. Sci., vol. NS-34, no. 6, pp. 1134-9, 1987.

[Taylo-92] E. W. Taylor, J, Berry, A. D. Sanchez, R. J. Padden, S. DeWalt, and S. Chapman, "First Operational Space Fiber Optic Data Links Orbited Aboard The Long Duration Exposure Facility-Lessons Learned,""1992 DOD Fiber Optics Conference Proceedings.

[Teag-72] M. J. Teague and E. G. Stassinopoulos, "A model of the Starfish Flux in the Inner Radiation Zone," X-601-72-487, NASA/GSFC, Greenbelt, MD, Dec. 1972.

[Thele-94] D. Thelen, S. Rankin, P. Marshall, K. A. LaBel, and M. Krainak, "A dual rate MIL-STD-1773 fiber optic transceiver for satellite applications," *Photonics for Space Environments II,* vol. SPIE-XX, 1994.

[Walt-91] R. J. Walters, S. R. Messenger, G. P. Summers, E. A. Burke, and C. J. Keavney, "Space radiation effects in InP solar cells," IEEE Trans. on Nucl. Sci., vol. NS-38, pp. 1153-9, 1991.

[Weis-90] J. D. Weiss, "The radiation response of a Selfoc microlens," *J. Lightwave Technol.*, vol. 8, no. 7, pp.1107-1109, 1990.

[Wicz-86] J. J. Wiczer, "Radiation hardened optoelectronic components: Detectors," *Proc. SPIE,* vol. 616, pp. 254-266, 1986.

[Xaps-98] M.A. Xapsos, G.P. Summers and E.A. Burke, "Probability model for peak fluxes of solar proton events," *IEEE Trans. Nucl. Sci.*, vol. NS-45, no.6, pp. 2948-2953, 1998.

[Zieg-84] J. F. Ziegler, J. P. Biersack, and U. Littmark, *The Stopping and Range of Ions in Solids.* New York: Pergamgon, 1884.